AD-A125 474

AD

TECHNICAL REPORT ARBRL-TR-02474

THEORETICAL CONSIDERATIONS IN MEASURING THE SIX-DEGREE-OF-FREEDOM MOTION OF GUN TUBES BY ACCELEROMETERS

James O. Pilcher II

February 1983

US ARMY ARMAMENT RESEARCH AND DEVELOPMENT COMMAND
BALLISTIC RESEARCH LABORATORY
ABERDEEN PROVING GROUND, MARYLAND

Approved for public release; distribution unlimited.

Additional copies of this report may be obtained from the National Technical Information Service, U. S. Department of Commerce, Springfield, Virginia 22161.

UNCLASSIFIED

SECURITY CLASSIFICATION OF THIS PAGE (When Data Entered)

REPORT DOCUMENTATION PAGE

READ INSTRUCTIONS BEFORE COMPLETING FORM

1. REPORT NUMBER: TECHNICAL REPORT ARBRL-TR-02474	2. GOVT ACCESSION NO.
	3. RECIPIENT'S CATALOG NUMBER
4. TITLE (and Subtitle): THEORETICAL CONSIDERATIONS IN MEASURING THE SIX-DEGREE-OF-FREEDOM MOTION OF GUN TUBES BY ACCELEROMETERS	5. TYPE OF REPORT & PERIOD COVERED: Technical Report
	6. PERFORMING ORG. REPORT NUMBER
7. AUTHOR(s): JAMES O. PILCHER II	8. CONTRACT OR GRANT NUMBER(s)
9. PERFORMING ORGANIZATION NAME AND ADDRESS: U.S. Army Ballistic Research Laboratory, ATTN: DRDAR-BLI, Aberdeen Proving Ground, MD 21005	10. PROGRAM ELEMENT, PROJECT, TASK AREA & WORK UNIT NUMBERS: 1L162618AH80, 1L161102AH43
11. CONTROLLING OFFICE NAME AND ADDRESS: U.S. Army Armament Research & Development Command, U.S. Army Ballistic Research Laboratory (DRDAR-BL), Aberdeen Proving Ground, MD 21005	12. REPORT DATE: February 1983
	13. NUMBER OF PAGES: 64
14. MONITORING AGENCY NAME & ADDRESS (if different from Controlling Office)	15. SECURITY CLASS. (of this report): UNCLASSIFIED
	15a. DECLASSIFICATION/DOWNGRADING SCHEDULE

16. DISTRIBUTION STATEMENT (of this Report)

Approved for public release; distribution unlimited

17. DISTRIBUTION STATEMENT (of the abstract entered in Block 20, if different from Report)

18. SUPPLEMENTARY NOTES

19. KEY WORDS (Continue on reverse side if necessary and identify by block number)

Six-Degree-Of-Freedom Analysis
Vector Analysis
Accelerations
Vector Transformation

20. ABSTRACT (Continue on reverse side if necessary and identify by block number) jmk

The second total derivative of the position vector, which describes the position of an accelerometer fixed to a body moving in space, is examined to determine the six-degrees-of-freedom acceleration vector. The dot product of the accelerometer response vector with the acceleration vector is examined to determine the spacial relationships required to separate vectorial components of acceleration and the effect of cross-axis sensitivity on the measurement of gun tube motion.

Basic array geometries are presented with the algorithms required to

DD FORM 1 JAN 73 1473 EDITION OF 1 NOV 65 IS OBSOLETE

UNCLASSIFIED

SECURITY CLASSIFICATION OF THIS PAGE (When Data Entered)

Continued

analyze the data for each array. Cross-axis sensitivity and data system response requirements are also discussed.

TABLE OF CONTENTS

TABLE OF CONTENTS (continued)

LIST OF ILLUSTRATIONS

LIST OF TABLES

I. INTRODUCTION

A. Background

Since the mid 1950's and especially the last five years, considerable effort has been expended by various DOD agencies, the Ballistic Research Laboratory being one, to measure the motion of gun tubes during the interior ballistic and launch cycle. The primary purpose of these measurements is to obtain correlations between gun system dynamic behavior and overall system accuracy. The secondary purpose is to validate numerical gun system simulations to predict system behavior. Although various measurement techniques have been tried with varying degrees of success, the use of accelerometers still holds the most promise, provided their measurement results can be unequivocally interpreted. The primary advantage of accelerometers is that they can be applied under field conditions with limited restriction or modification of the gun system.

B. The Basic Problem

The basic problem is to measure the components of dynamic motion of the gun tube that significantly affect the launch conditions of the projectile and its subsequent terminal accuracy. The measurement problem becomes one of being able to discern the significant vector components of motion at a point on the gun tube from a complex combination of vector components generated by various dynamic phenomena, including the ones of interest. Unlike well-controlled laboratory experiments designed to separate various physical phenomena, gun system acceleration measurements are subject to interference from local accelerations generated by stress waves, dilational vibrations, traveling loads, impulsive forces and unbalanced projectiles.

C. Approach to the Problem

To gain a meaningful measurement from accelerometers, one must take advantage of the characteristics of the physical phenomena encountered during the measurement. Remembering that the global structural motion is paramount, emphasis is placed on the low-frequency response of the system. By separating analytically and by appropriate filtering, the high-frequency interference can be eliminated from the measurement. Separation of the desired vector components of motion is achieved through the judicious design of sensor arrays based on vector mechanics.

1. Fourier Analysis and Cross Correlation Technique. These techniques are applied during the data analysis and rely on the spectral nature of the physical phenomena being measured to facilitate separation of effects.[1] The viability of these techniques is strengthened by proper sensor array design and filtering techniques.

2. Mechanical and Electronic Filtering Techniques. By mechanical filtering between the sensor and the phenomena and electronic filtering between the sensor and the acquisition system, undesirable high frequency physical effects can be separated from the measurement. This allows greater sensitivity to be achieved in the measurement with increased sensor reliability and decreased burden on the analysis. However, these techniques must be carefully designed for the specific phenomena to be measured and for the specific system on which the measurement is made.[2,3]

3. Spacial Arrays and Vector Discrimination Techniques. To implement a viable acceleration measurement in a six-degree-of-freedom environment, sensors must be mounted in a spacial array in order to discriminate and separate the desired vector components from the measured data. The

---

[1] *James N. Walbert, "Application of Digital Filters and the Fourier Transform to the Analysis of Ballistic Data," BRL Technical Report ARBRL-TR-02347, 1981 (ADA 102890).*

[2] *James N. Walbert, "Computer Algorithms for the Design and Implementation of Linear Phase Finite Impulse Response Digital Filters," BRL Technical Report ARBRL-TR-02346, 1981 (ADA 103112).*

[3] *James O. Pilcher II, "Application of Mechanical Filters to Ballistic Measurements," BRL Technical Report (to be published)*

application of these techniques governs the required analyses techniques and enhances the efficiency of filtering techniques.

The remainder of this report discusses the analytical rationale behind the design of spacial arrays to facilitate separation of the vector components of gun tube motion. The other techniques mentioned above will be discussed in subsequent reports.

II. SIX-DEGREE-OF-FREEDOM MOTION OF A POINT ON A GUN TUBE

In order to design an accelerometer array for measuring the motion of a gun tube, a description of the motion of the point of measurement is required. Once such a description is achieved, arrays can be designed to enhance or minimize certain vector components of acceleration as desired. Naturally, any such description must rely on assumptions about the behavior of the gun tube.

A. Assumptions

The following are the basic assumptions about the behavior of a gun tube and the resulting motion at a point on the surface of the gun tube.

1. Cross-Sectional Property. A plane cross section of the gun tube remains planar throughout the duration of the dynamic response of the gun tube. This assumes that local bending deformations are very small and elastic. Phenomena that violate this assumption are passage of a cocked projectile, load or geometric discontinuities in the immediate vicinity of the point of measurement and unbalanced projectiles. Figure 1 illustrates this assumption.

2. In-Plane Behavior of The Cross Section. The cross section of the gun tube can undergo both symmetrical and asymmetrical deformation about the central axis in the plane of the cross section. This assumption allows assessment of the acceleration components generated by dilational vibration, ovality due to local bending, Bourdon effects and projectile passage. Figure 2 illustrates this assumption.

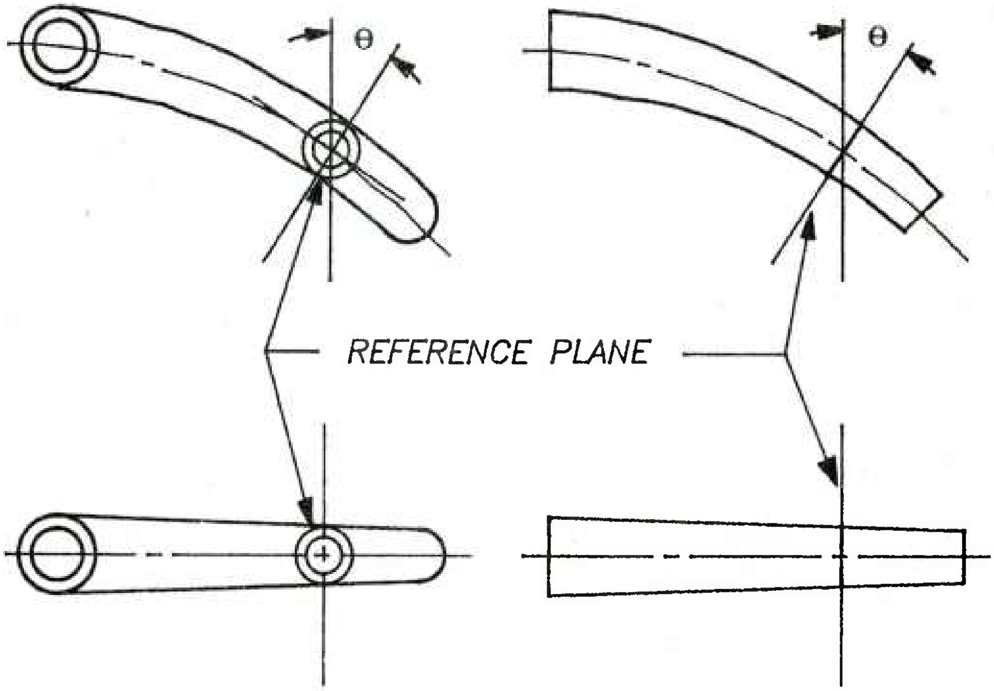

Figure 1. Planar Properties of a Gun Tube

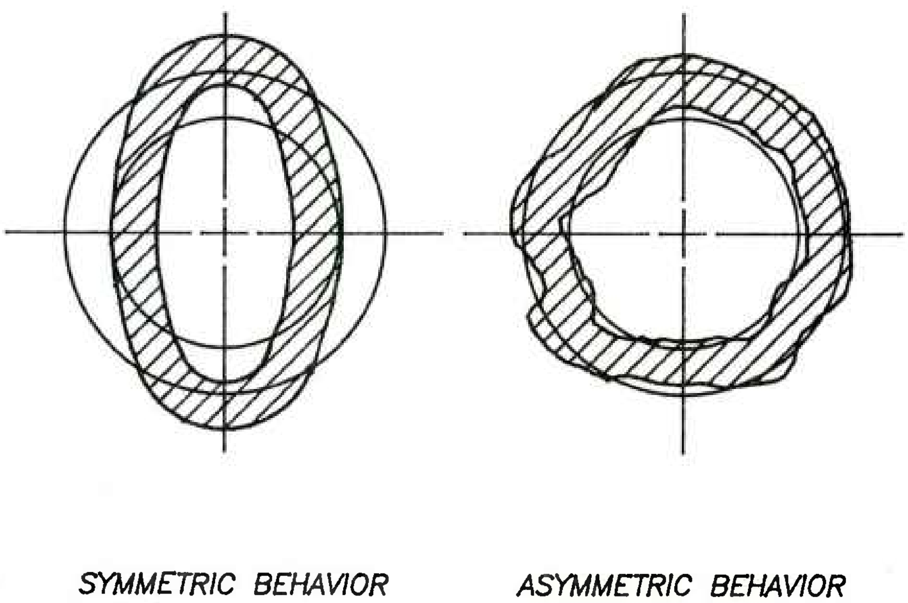

Figure 2. In-Plane Behavior of a Gun Tube

3. <u>Local Coordinate System</u>. The local coordinate system is assumed to be Cartesian, fixed with respect to the cross-section plane, with two of the axes lying in the plane and the origin at the center line of the tube. This coordinate system translates and rotates with respect to a fixed Earth coordinate system. Consequently, any vector that is directionally fixed in the plane of the cross section has a time derivative of the unit vectors due to their changes in direction. Figure 3 illustrates this assumption.

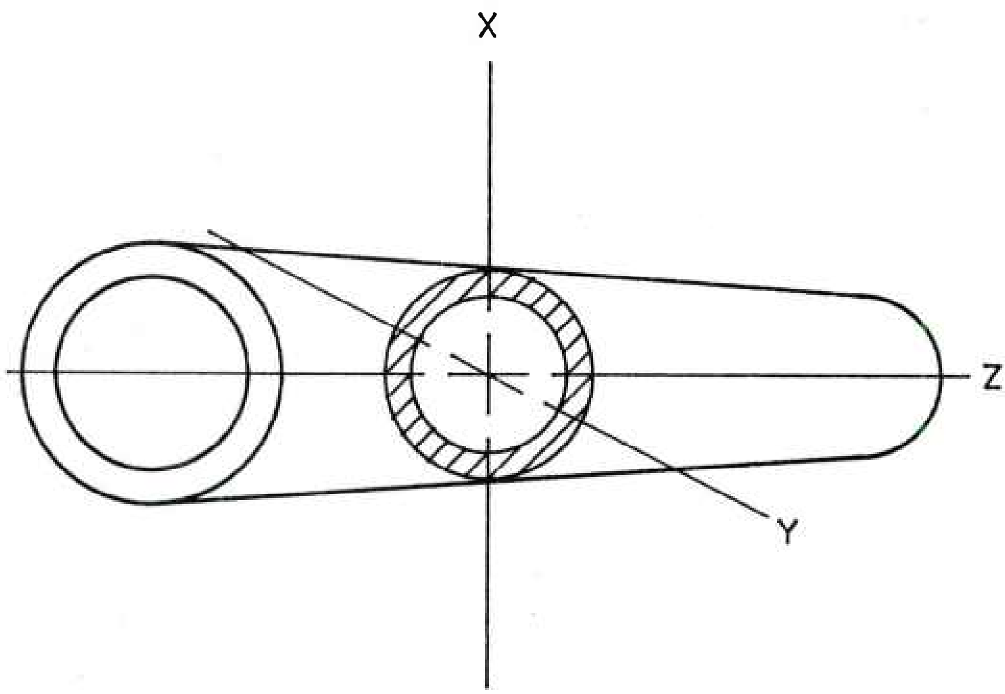

Figure 3. Local Coordinate System

4. <u>Continuity</u>. The motion is assumed to have a continuous second time derivative. That is, the third time derivative is defined and bounded except at discrete points where it possesses left- and right-hand limits. This assumption is based on the gun structure conforming to the laws of classical mechanics of rigid and deformable bodies. Deviations from this assumption would be indicative of failure of a structural component or the sensor.

5. <u>Inertial Reference</u>. Since accelerometers are inertial devices, the measurement constitutes an observation from a point displaced away from the

center of rotation of a body moving through space. The sensed accelerations, then, are the components of the translational motion dependent on the instantaneous angle of rotation of the local coordinate system with respect to the Earth coordinate system, in conjunction with the cross products of the local displacement vector with the angular rates of change of the local coordinate system.[4]

B. Position Vector

The position of the point of measurement on the outer surface of the gun tube is described in terms of the unit vectors $\overline{U}_x$, $\overline{U}_y$ and $\overline{U}_z$ of the local coordinate system by the position vector,

$$\overline{P} = \overline{R} + \overline{r} \,, \tag{1}$$

where $\overline{R}$ = the radius vector emanating from the origin of the Earth coordinate system and terminating at the origin of the local coordinate system.

$\overline{r}$ = the radius vector emanating from the origin of the local coordinate system and terminating at the point of measurement.

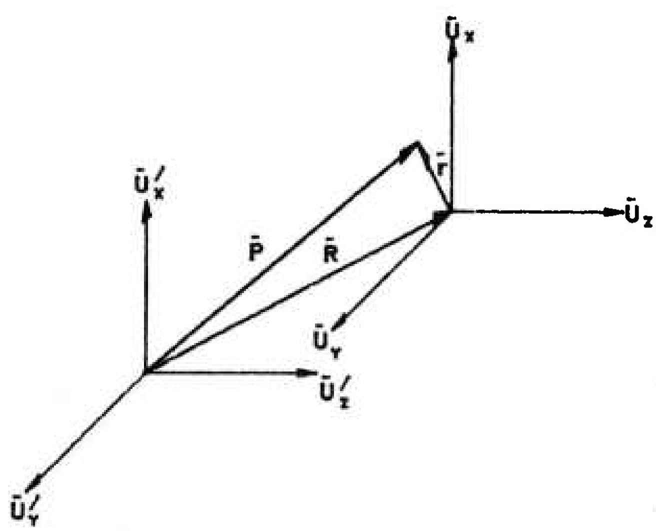

Figure 4. Position Vector

---

[4] *S.W. McCuskey, Introduction to Advanced Dynamcis, Addison-Wesley Publishing Company, 1958.*

In expanded form,

$$\bar{P} = (R_x+r_x)\ \bar{U}_x + (R_y+r_y)\ \bar{U}_y + (R_z+r_z)\ \bar{U}_z. \tag{2}$$

C. Velocity Vector

The velocity at the point of measurement on the tube is obtained by forming the total time derivative of the position vector. Bear in mind that the derivative of the unit vector $\bar{U}$ exists because of the rotation of the local coordinate system and is

$$\frac{d\bar{U}}{dt} = \bar{\omega} \times \bar{U}$$

where $\bar{\omega}$ = the angular rate of change of $\bar{U}$ which is of constant magnitude

Therefore,

$$\bar{V} = \frac{d\bar{P}}{dt} = \dot{\bar{R}} + \dot{\bar{r}} + \bar{\omega} \times (\bar{R} + \bar{r}) \tag{3}$$

where

$\bar{\omega}$ = the time rate of change of the local coordinate system;

$\bar{\omega} \times \bar{r}$ = is the velocity normal to the position vector, r.

In expanded form,

$$\bar{V} = [\dot{R}_x+\dot{r}_x + (R_z+r_z)\omega_y - (R_y+r_y)\omega_z]\bar{U}_x$$

$$+ [\dot{R}_y+\dot{r}_y + (R_x+r_x)\omega_z - (R_z+r_z)\omega_x]\bar{U}_y$$

$$+ [\dot{R}_z+\dot{r}_z+(R_y+r_y)\omega_x - (R_x+r_x)\omega_y]\bar{U}_z \qquad (4)$$

The term $\dot{\bar{r}}$ in Eq. (3) results from the flexibility of the tube cross section and vanishes for a rigid cross section. Figure 5 illustrates the velocity vector, $\bar{V}$.

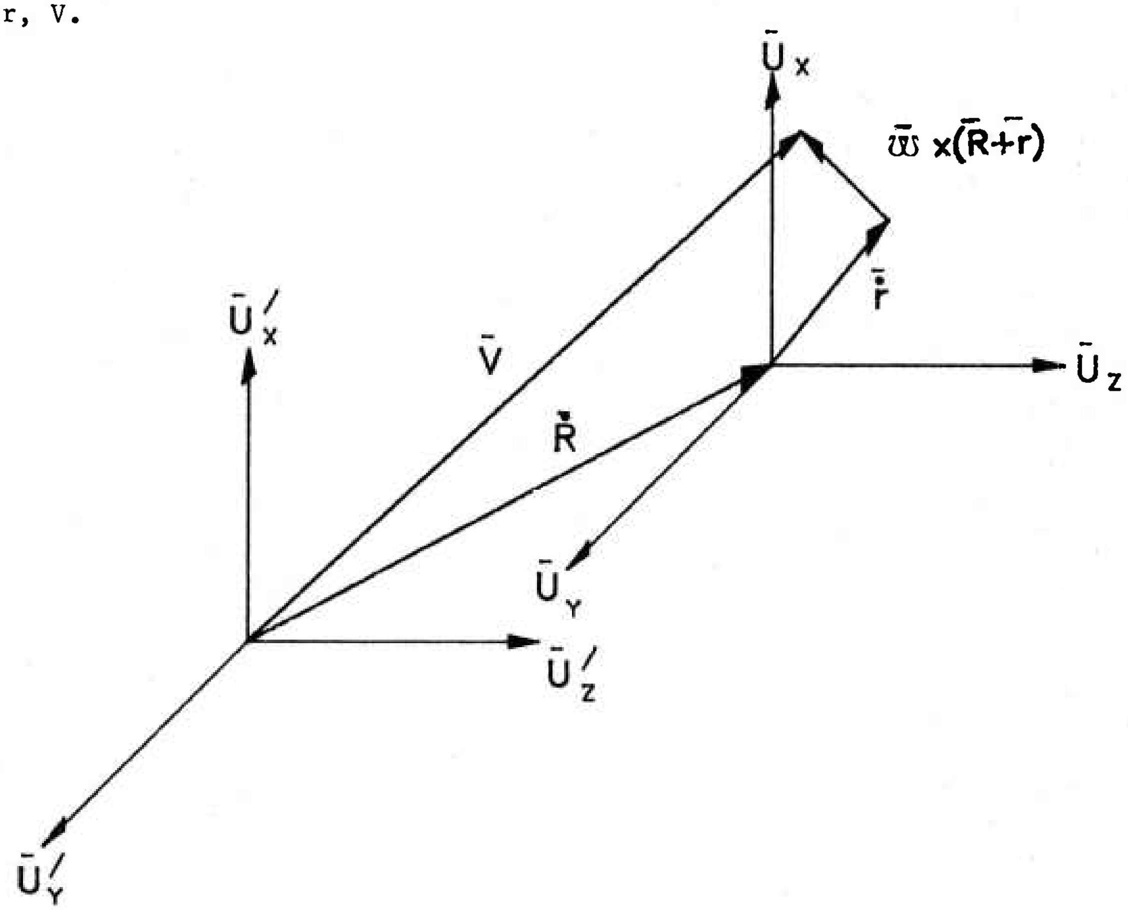

Figure 5. Velocity Vector

D. Acceleration Vector

The acceleration vector is the total time derivative of the velocity vector, $\bar{V}$.

$$\bar{A} = \frac{d\bar{V}}{dt} = \frac{d\dot{\bar{R}}}{dt} + \frac{d\dot{\bar{r}}}{dt} + \frac{d\left((\bar{\omega}x(\bar{R}+\bar{r})\right)}{dt} .$$

$$\bar{A} = \ddot{\bar{R}} + \ddot{\bar{r}} + 2(\bar{\omega}x(\dot{\bar{R}}+\dot{\bar{r}}) + \bar{\omega}(\bar{\omega}\cdot(\bar{R}+\bar{r}))-(\bar{R}+\bar{r})(\bar{\omega}\cdot\bar{\omega}) + \dot{\bar{\omega}}x(\bar{R}+\bar{r}) . \tag{5}$$

where

$2(\bar{\omega}x(\dot{\bar{R}}+\dot{\bar{r}})) + \bar{\omega}(\bar{\omega}\cdot\bar{R}+\bar{r}) - (\bar{R}+\bar{r})(\bar{\omega}\cdot\bar{\omega})$ is the coriolis accelerations;

$\dot{\bar{\omega}}x(\bar{R}+\bar{r})$ is the tangential accelerations.

In expanded form,

$$\begin{aligned}
\bar{A} = {} & [\ddot{R}_x+\ddot{r}_x+\omega_x\omega_y(R_y+r_y)+\omega_x\omega_z(R_z+r_z)-(R_x+r_x)(\omega_y^{\,2}+\omega_z^{\,2}) \\
& + 2\omega_y(\dot{R}_z+\dot{r}_z)-2\omega_z(\dot{R}_y+\dot{r}_y)+\dot{\omega}_y(R_z+r_z)-\dot{\omega}_z(R_y+r_y)]\bar{U}_x \\
& + [\ddot{R}_y+\ddot{r}_y+\omega_y\omega_z(R_z+r_z)+\omega_y\omega_x(R_x+r_x)-(R_y+r_y)(\omega_z^{\,2}+\omega_x^{\,2}) \\
& + 2\omega_z(\dot{R}_x+\dot{r}_x)-2\omega_x(\dot{R}_z+\dot{r}_z)+\dot{\omega}_z(R_x+r_x)-\dot{\omega}_x(R_z+r_z)]\bar{U}_y \\
& + [\ddot{R}_z+\ddot{r}_z+\omega_z\omega_x(R_x+r_x)+\omega_z\omega_y(R_y+r_y)-(R_z+r_z)(\omega_x^{\,2}+\omega_y^{\,2}) \\
& + 2\omega_x(\dot{R}_y+\dot{r}_y)-2\omega_y(\dot{R}_x+\dot{r}_x)+\dot{\omega}_x(R_y+r_y)-\dot{\omega}_y(R_x+r_x)]\bar{U}_z
\end{aligned} \tag{6}$$

The expanded acceleration equation, Eq. (6), demonstrates the problem of separating specific vector components. For studying and determining accuracy effects, the vector components, ω, $\bar{R}$, $\dot{R}$, in terms of the Earth coordinate system, are generally the primary components of interest. These vectors are derived by attempting to separate and transform $\ddot{\bar{R}}$ and $\ddot{\bar{\omega}}$ and evaluating their subsequent integrals. These components are often used to verify numerical simulation results. Rather than follow these techniques, a different approach is in order.

The angular velocity square terms and the inner product of angular velocity constitute the products of frequency terms which generate beats and second harmonics. This means that measurement and acquisition system bandwidths and data rates must be commensurate for frequency response twice as high as those predicted by normal mode analyses.

E. Some Simplifications

Before progressing further an examination of the terms in Eq. (6) is in order. By rearranging Eq. (6) and substituting

$$M_x = [\ddot{R}_x+\omega_x\omega_y R_y+\omega_x\omega_z R_z-R_x(\omega_y^2+\omega_z^2)+2\omega_y\dot{R}_z-2\omega_z\dot{R}_y+\dot{\omega}_y R_z-\dot{\omega}_z R_y];$$

$$M_y = [\ddot{R}_y+\omega_y\omega_z R_z+\omega_y\omega_x R_x-R_y(\omega_z^2+\omega_x^2)+2\omega_z\dot{R}_x-2\omega_x\dot{R}_z+\dot{\omega}_z R_x-\dot{\omega}_x R_z] ;$$

$$M_z = [\ddot{R}_z+\omega_z\omega_x R_x+\omega_z\omega_y R_y-R_z(\omega_x^2+\omega_y^2)+2\omega_x\dot{R}_y-2\omega_y\dot{R}_x+\dot{\omega}_x R_y-\dot{\omega}_y R_x] ;$$

$$\begin{aligned}\bar{A} = {} & [M_x+\ddot{r}_x+\omega_x\omega_y r_y+\omega_x\omega_z r_z-r_x(\omega_y^2+\omega_z^2)+2\omega_y\dot{r}_z-2\omega_z\dot{r}_y+\dot{\omega}_y r_z-\dot{\omega}_z r_y]\bar{U}_x \\ & + [M_y+\ddot{r}_y+\omega_y\omega_z r_z+\omega_y\omega_x r_x-r_y(\omega_z^2+\omega_x^2)+2\omega_z\dot{r}_x-2\omega_x\dot{r}_z+\dot{\omega}_z r_x-\dot{\omega}_x r_z]\bar{U}_y \\ & + [M_z+\ddot{r}_z+\omega_z\omega_x r_x+\omega_z\omega_y r_y-r_z(\omega_x^2+\omega_y^2)+2\omega_x\dot{r}_y-2\omega_y\dot{r}_x+\dot{\omega}_x r_y-\dot{\omega}_y r_x]\bar{U}_z \end{aligned} \quad (7)$$

The terms M_x, M_y, M_z are the components of relative motion between the origins of the Earth and local coordinate systems.

Eq. (7) can be immediately simplified by applying the previous assumptions. Since the measuring point lies in the same plane as the origin and two axes of the local coordinate system, its description becomes two-dimensional. As a matter of convention, the coordinate axes often used are the x axis in the vertical direction, the y axis in the horizontal direction and the z axis perpendicular to the x-y plane and tangent to the axis of the gun tube at its intersection with the x-y plane. This means that the tube cross section at the point of measurement lies in the x-y plane and that the r_z component of the position vector has zero magnitude. This immediately simplifies Eq. (7) to that shown in Eq. (8).

$$\begin{aligned}\bar{A} = {} & [M_x+\ddot{r}_x+\omega_x\omega_y r_y-r_x(\omega_y{}^2+\omega_z{}^2)-2\omega_z\dot{r}_y-\dot{\omega}_y r_y]\bar{U}_x \\ & [M_y+\ddot{r}_y+\omega_y\omega_x r_x-r_y(\omega_y{}^2+\omega_z{}^2)+2\omega_z\dot{r}_x+\dot{\omega}_z r_x]\bar{U}_y \\ & [M_z+\omega_z\omega_x r_x+\omega_z\omega_y r_y+2\omega_x\dot{r}_y-2\omega_y\dot{r}_x+\dot{\omega}_x r_y-\dot{\omega}_y r_x]\bar{U}_z\end{aligned} \tag{8}$$

When the sensor is placed on either the x or y axis, Eq. (7) reduces to Eqs. (9) and (10). When the sensor is on the y axis, r_x, $\dot{r}_x$ and $\ddot{r}_x$ are equal to 0; thus

$$\begin{aligned}\bar{A} = {} & [M_x+\omega_x\omega_y r_y-2\omega_z\dot{r}_y-\dot{\omega}_z r_y]\bar{U}_x \\ & + [M_y+\ddot{r}_y-r_y(\omega_y{}^2+\omega_z{}^2)]\bar{U}_y \\ & + [M_z+\omega_z\omega_y r_y+2\omega_x\dot{r}_y+\dot{\omega}_x r_y]\bar{U}_z\end{aligned} \tag{9}$$

When the sensor is on the x axis, r_y, $\dot{r}_y$ and $\ddot{r}_y$ equal 0; thus,

$$
\begin{aligned}
\bar{A} &= [\ddot{M}_x+\ddot{r}_x-r_x(\omega_y{}^2+\omega_z{}^2)]\bar{U}_z \\
&+ [M_y+\omega_y\omega_x r_x+2\omega_z\dot{r}_x+\dot{\omega}_z r_x]\bar{U}_y \\
&+ [M_z+\omega_z\omega_x r_x-\omega_y\dot{r}_x-\dot{\omega}_y r_x)\bar{U}_z .
\end{aligned}
\tag{10}
$$

Further simplification can be achieved by taking advantage of the character of the position vector $\bar{r}$. Two types of motion occur in the cross section of the tube, symmetrical and asymmetrical. Both of these types of motion are radial deflections induced by local strain effects that tend to be much higher in frequency than the structural response. Though these displacements are small enough to ignore, their corresponding accelerations are quite intense. These phenomena, with the exception of the impulse generated by projectile passage through the plane, generate high-frequency and high-intensity oscillating accelerations. These oscillations are in excess of 2 kg's in amplitude and above 7 kHz in frequency. Consequently, these oscillations can be eliminated from the data by mechanical filtering between the sensor and the gun tube. The vector $\bar{r}$ can be recast as

$$
\bar{r} = \bar{d} + \bar{\delta} + \bar{\zeta}, \tag{11}
$$

where

$\bar{d}$ = gun tube radius in plane of measurement and is of constant length;

$\bar{\delta}$ = oscillatory displacement about the length of $\bar{d}$;

$\bar{\zeta}$ = impulsive displacement about $\bar{d}$.

The impulse displacement ζ can often be separated by Fourier techniques during the data analyses. Thus, by eliminating the effects $\bar{\delta}$ and $\bar{\zeta}$ from vector $\bar{r}$, Eqs. (9) and (10) reduce to Eqs. (12).

For $\bar{r} = r_x \bar{U}_x$,

$$\bar{A} = [M_x - r_x(\omega_y^2 + \omega_z^2)]\bar{U}_x + [M_y + \omega_y \omega_x r_x + \dot{\omega}_z r_x]\bar{U}_y + [M_z + \omega_z \omega_x r_x - \dot{\omega}_y r_x]\bar{U}_z \;;$$

for $\bar{r} = r_y \bar{U}_y$,

$$\bar{A} = [M_x + \omega_x \omega_y r_y - \dot{\omega}_z r_y]\bar{U}_x + [M_y - r_y(\omega_y^2 + \omega_z^2)]\bar{U}_y + [M_z + \omega_z \omega_y r_y + \dot{\omega}_x r_y]\bar{U}_z \;. \tag{12}$$

Further simplification of the problem involves sensor selection and directional properties.

III. GENERAL EQUATION FOR ACCELEROMETER RESPONSE

Accelerometers are not unidirectional[5] devices; their response is three dimensional in character. Because most accelerometer measurements are performed under conditions of relatively unidirectional excitation such as vibration and shock machines, the assumption of unidirectionality is often made without appreciably degrading the measurement. However, under the conditions arising from gun and projectile dynamics, such an assumption is very misleading and can cause considerable degradation of the measurement. In fact, most measurements cannot be made without taking advantage of the three-

[5] *Charles C. Crede and Cyril M. Harris, Shock and Vibration Handbook, Volume 1, McGraw-Hill, 1961.*

dimensional character of the accelerometer. In order to establish a viable relationship for accelerometer sensitivity, the vector characteristics of the sensing element, its misalignments with external reference surfaces and local coordinate systems must be considered.

A. Accelerometer Response Characteristics

Assuming that the accelerometer is subjected to an environment within its capabilities in both the magnitude and frequency domain, its response characteristics can be expressed as a vector $\bar{S}(\sigma,\bar{\tau},\bar{\pi})$ where $\bar{\sigma}$, $\bar{\tau}$, $\bar{\pi}$, are the unit vectors of the sensor coordinate system. This coordinate system is not necessarily orthogonal, but the deviations from orthogonality are generally very small angles. In addition, there generally exist small rotations of the principal components of the sensitivity vector with respect to the external reference system of the device. The angles of rotation and nonorthogonality are sufficiently small to be lumped together in the direction angles $\bar{\alpha}$, $\bar{\beta}$, $\bar{\gamma}$. By performing an orthogonal transformation,[6] the components of sensitivity can be expressed in terms of an orthogonal coordinate system with unit vectors $\bar{x}$, $\bar{y}$ and $\bar{z}$ which are referenced to the external geometry of the device. Figure 6 illustrates the relationships of these coordinate systems. Figure 7 shows a comparison of an ideal accelerometer response surface with a realistic response surface.

The external sensor geometry is generally defined as having a principal axis that will be defined as being colinear with $\bar{z}$ and a mounting surface that is a plane either normal or parallel to the principal axis. In our discussions, we will address the normal plane case. Another condition placed on the analysis is that $\bar{x}$ lies in the plane defined by $\bar{\pi}$ and $\bar{\sigma}$. This condition can be readily established from calibration data. The sensitivity vector is defined as

---

[6] *Richmond B. McQuistan, Scalar and Vector Fields, John Wiley & Sons, 1965.*

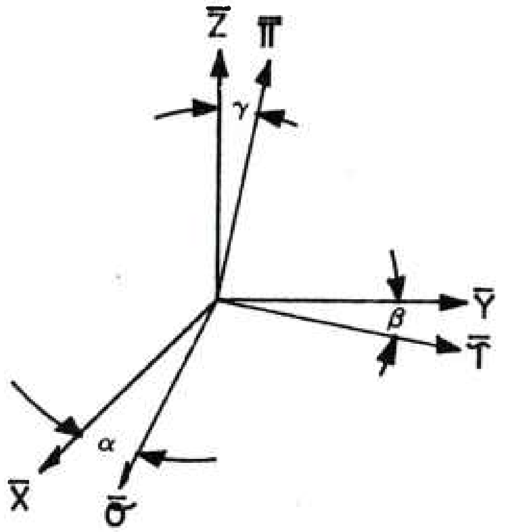

Figure 6. Geometrical and Sensing Coordinates

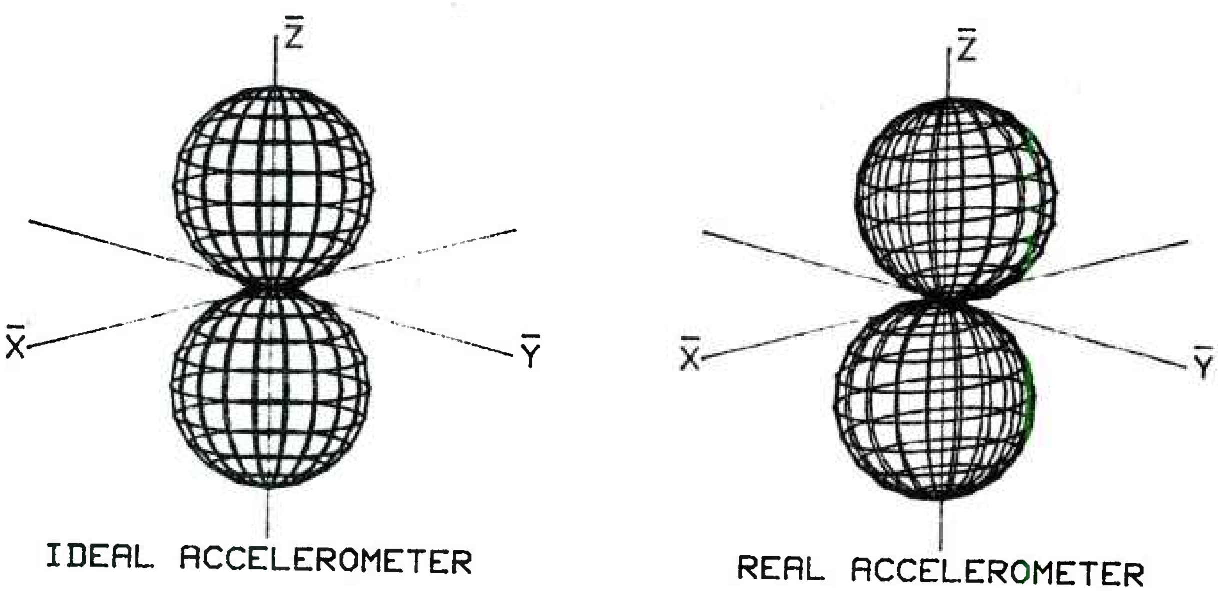

Figure 7. Sensitivity Surfaces for Ideal and Real Accelerometers

$$\bar{S} = S\bar{\sigma}+T\bar{\tau}+P\bar{\pi}=(a_{x\sigma}S+a_{x\tau}T+a_{x\pi}P)\bar{x}+(a_{y\sigma}S+a_{y\tau}T+a_{y\pi}P)\bar{y} \tag{13}$$

$$+(a_{z\sigma}S+a_{z\tau}T+a_{z\pi}P)\bar{z},$$

where

a_{ij} = is the direction cosine between unit vector i and unit vector j.

Eq. (13) is only applicable when α, β, γ are sufficiently small such that $\sin(\alpha)=\alpha$, $\sin(\beta)=\beta$ and $\sin(\gamma)=\gamma$ and $\cos(\alpha)=1$, $\cos(\beta)=1$ and $\cos(\gamma)=1$. General measurement accuracy dictates that these angles should be less than 3.4 degrees or 0.06 radian. Table 1 gives the transformation coefficients.

TABLE 1. TRANSFORMATION COEFFICIENTS (A_{ij})

	$\bar{\sigma}$	$\bar{\tau}$	$\bar{\pi}$
$\bar{x}$	1	$-\beta$	α
$\bar{y}$	β	1	$-\gamma$
$\bar{z}$	$-\alpha$	γ	1

Eq. (13) then becomes

$$\bar{S} = (S-\beta T+\alpha P)\bar{x}+(\beta S+T-\gamma P)\bar{y}+(-\alpha S+\gamma T+P)\bar{z}. \tag{14}$$

Eq. (14) can be stated with simpler coefficients relatable to the cross-axis sensitivities as measured during calibration.

$$\bar{S} = Pk_1\bar{x} + Pk_2\bar{y} + P\bar{z}. \tag{15}$$

where

P = primary sensitivity in units/g;

k_1 = maximum cross-axis sensitivity in %/100;

k_2 = value of cross-axis sensitivity orthogonal to k_1 in %/100.

For some accelerometers which have nearly perfect alignment, $k_1 = k_2$

$$\bar{S} = Pk_1\bar{x} + Pk_1\bar{y} + P\bar{z}. \tag{16}$$

For an ideal accelerometer k_1 and k_2 are zero; thus,

$$\bar{S} = P\bar{z}. \tag{17}$$

The conditions in Eq. (16) are often found by screening accelerometers with less than 1% cross-axis sensitivity. The conditions in Eq. (17) have been approached by some piezoresistive accelerometers, but not without degrading some other properties. Eqs. (15), (16) and (17) show that calibrations describing the behavior in three orthogonal planes are required for six-degree-of-freedom measurements. The remainder of our discussion will use Eq. (15) as the basis of analysis.

B. Accelerometer Mount Misalignment

The misalignment of accelerometer axes due to mounting conditions can introduce significant error into the measurement. For accelerometers that are bonded or fastened to their mounting surface by external means, mounting error can be eliminated by the use of precision fixtures and techniques during the mounting process. However, stud mounted accelerometers limit the ability to align the transverse axis in the desired direction. This type of misalignment often causes large angles of rotation and requires a different correction technique than the first type mentioned.

1. Bonded Accelerometer. Although precision fixtures and techniques are used in the mounting process, misalignments do occur due to human error. Errors resulting from such misalignments can be corrected by the same type of transformation discussed in the previous section. Figure 8 shows the accelerometer coordinates misaligned with the local coordinate system.

$$\bar{S}(\bar{x},\bar{y},\bar{z}) = \bar{S}(\bar{U}_1,\bar{U}_2,\bar{U}_3) \tag{18}$$

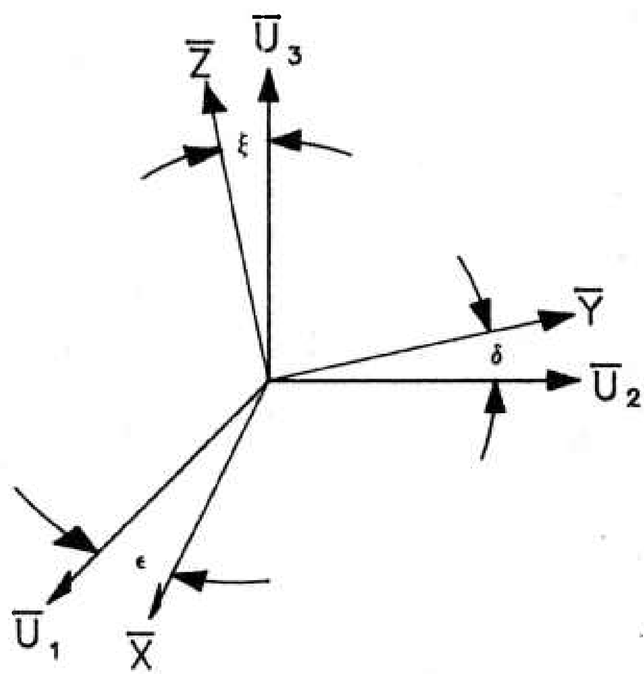

Figure 8. Mounting Misalignment for Bonded Accelerometer

Table 2 shows the transformation coefficients for the angles ε, δ, ξ shown in Figure 8.

TABLE 2. TRANSFORMATION COEFFICIENTS (ε, δ, ξ)

	$\bar{x}$	$\bar{y}$	$\bar{z}$
$\bar{U}_1$	1	$-\varepsilon$	$-\xi$
$\bar{U}_2$	ε	1	δ
$\bar{U}_3$	ξ	$-\delta$	1

$$\bar{S} = P(k_1-\varepsilon k_2-\xi)\bar{U}_1+P(\varepsilon k_1+k_2+\delta)\bar{U}_2+P\ (\xi k_1-\delta k_2+1)\bar{U}_3, \tag{19}$$

or,

$$\bar{S} = a\bar{U}_1+b\bar{U}_2+c\bar{U}_3, \tag{20}$$

where

$a = P(k_1- \varepsilon k_2- \xi);$

$b = P(\varepsilon k_1+ k_2+ \delta);$

$c = P(\xi k_1- \delta k_2+1).$

2. <u>Stud Mounted Accelerometers</u>. Stud mounted accelerometers pose the problem that the final alignment of the accelerometer may include a large angle of misalignment which is usually in the cross-axis plane. Because of the large angle, a two-step transformation is required. First, an arbitrary local coordinate system is assumed with one of its unit vectors colinear with the maximum cross-axis sensitivity vector as shown in Figure 9. An orthogonal transformation is performed resolving $\bar{S}(\bar{x},\bar{y},\bar{z})$ into $S(\bar{U}_1',\bar{U}_2',\bar{U}_3')$. Table 3 gives the coefficients of this transformation.

TABLE 3. TRANSFORMATION COEFFICIENTS (ε=0)

	$\bar{x}$	$\bar{y}$	$\bar{z}$
$\bar{U}_1'$	1	0	$-\xi$
$\bar{U}_2'$	0	1	δ
$\bar{U}_3'$	ξ	$-\delta$	1

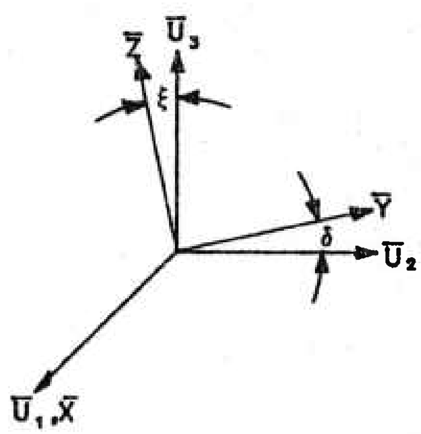

Figure 9. Mounting Misalignment for Stud Mounted Accelerometer to Adjusted Local Coordinates

The transformed vector is

$$\bar{S} = P(k_1-\xi)\bar{U}_1+P(k_2+\delta)\bar{U}_2 + P(\xi k_1-\delta k_2+1)\bar{U}_3. \tag{21}$$

The second step is to perform the transformation of the rotation of the large angle ε about $\bar{U}_3$ which is colinear with $\bar{U}_3'$ as shown in Figure 10. $\bar{U}_1$, $\bar{U}_2$, $\bar{U}_3$ are the local coordinates. Since angle ε is large, $\cos(\varepsilon) \neq 1$ and $\sin(\varepsilon) \neq \varepsilon$. The coefficients for this transformation are given in Table 4.

TABLE 4. TRANSFORMATION COEFFICIENTS FOR LARGE ε

	$\bar{U}_1'$	$\bar{U}_2'$	$\bar{U}_3'$
$\bar{U}_1$	$\cos(\varepsilon)$	$-\sin(\varepsilon)$	0
$\bar{U}_2$	$\sin(\varepsilon)$	$\cos(\varepsilon)$	0
$\bar{U}_3$	0	0	1

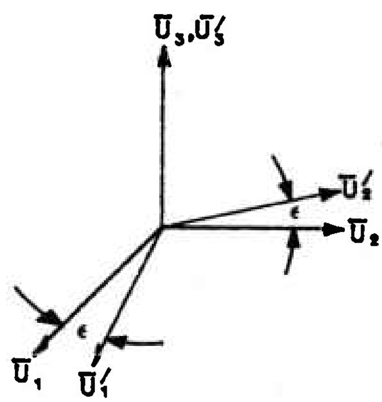

Figure 10. Mounting Misalignment for Stud Mounted Accelerometer to Local Coordinate System

$$\bar{S} = P[(k_1-\xi)\cos(\varepsilon)-(k_2+\delta)\sin(\varepsilon)]\bar{U}_1$$
$$+ P[(k_1-\xi)\sin(\varepsilon)+(k_2+\delta)\cos(\varepsilon)]\bar{U}_2$$
$$+ P(\xi k_1-\delta k_2 + 1)\bar{U}_3, \tag{22}$$

or,

$$\bar{S} = a\bar{U}_1 + b\bar{U}_2 + c\bar{U}_3, \tag{23}$$

where $a = P[(k_1-\xi)\cos(\varepsilon) - (k_2+\delta)\sin(\varepsilon)]$;

$b = P[(k_1-\xi)\sin(\varepsilon) + (k_2+\delta)\cos(\varepsilon)]$;

$c = P(\xi\delta k_1-\delta k_2+1)$.

IV. ACCELEROMETER ARRAYS

To facilitate separation of vector components, accelerometers must be arranged in distinct arrays about the plane of measurement for a specific situation. This allows the generation of sets of vector equations required to separate components.

Particular interest is paid to the separation of the relative acceleration term M_x, M_y and M_z. These terms are the structural response terms that are predicted by gun simulation programs. The terms involving products of r, $\dot{r}$ and $\ddot{r}$ are local effects generated by local strains which create accelerations that mask the measurand and also cause nonlinear response of the sensor. The strains caused by wave propagation are removed by mechanical filtering techiques. Other high-frequency phenomena can be removed by electronic methods; however, low frequency variations in r, particularly due to projectile passage, must be separated by comparative measurement of different positions in an array.

A. Single-Pair Array

The basic array is a pair of accelerometers displaced in space and oriented to specific directions. Although the convenience of symmetry is used in this analysis, it is not necessary and can be circumvented by analysis. The illustration in Figure 11 shows a pair of accelerometers mounted diametrically opposite one another on the surface of the gun tube. The origins of their coordinate systems lie in the plane of the cross section with their unit vectors parallel to the coordinate system of the cross section and antiparallel to each other. The displacement vectors to the center of the local coordinates from the center of the tube cross section are $\bar{r}_1$ and $\bar{r}_3$.

When

$\bar{r}_1 = r_1\bar{U}_x$, the acceleration vector is

$$\bar{A} = [M_x+\ddot{r}_1-r_1(\omega_y^2+\omega_z^2)]\bar{U}_x+[M_y+\omega_y\omega_x r_z+2\omega_z\dot{r}_1+\dot{\omega}_z r_1]\bar{U}_y+[M_z+\omega_z\omega_x r_1-\omega_y\dot{r}_1-\dot{\omega}_y r_1]\bar{U}_z \tag{24}$$

When

$\bar{r}_3 = r_3\bar{U}_x = - r_1\bar{U}_x$, the acceleration vector is

$$\bar{A} = [M_x-\ddot{r}_1+r_1(\omega_y^2+\omega_z^2)]\bar{U}_x+[M_y-\omega_y\omega_x r_1-2\omega_z\dot{r}_1-\dot{\omega}_z r_1]\bar{U}_y+[M_y-\omega_z\omega_x r_1+\omega_y\dot{r}_1+\dot{\omega}_y r_1]\bar{U}_z \tag{25}$$

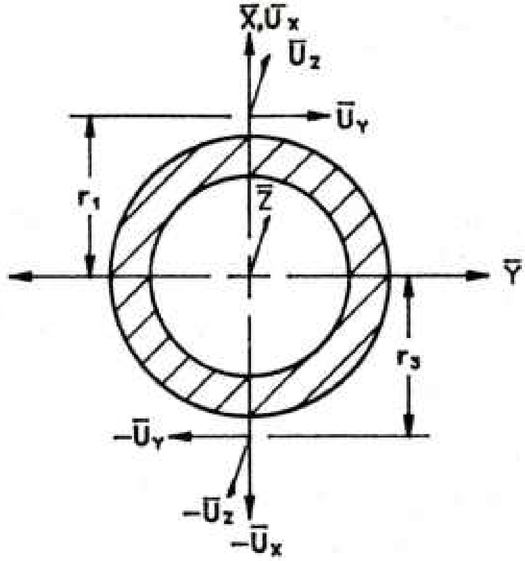

Figure 11. Single-Pair Array

The sensitivity vectors for the accelerometer can be expressed as

$$\bar{S}_i=(a_i\bar{U}_x + b_i\bar{U}_y + c_i\bar{U}_z). \tag{26}$$

The outputs are the dot product of the sensitivity vectors with their respective acceleration vectors.

$$O_i=\bar{S}_i\bullet\bar{A}_i \tag{27}$$

Since the coordinates at position 1 are parallel to the local coordinate system and the coordinates at position 3 are antiparallel to the local coordinate system,

$$\bar{S}_1 = a_1\bar{U}_x + b_1\bar{U}_y + c_1\bar{U}_z; \tag{28}$$

$$\bar{S}_3 = - a_3\bar{U}_x - b_3\bar{U}_y - c_3\bar{U}_z; \tag{29}$$

and

$$0_1 = a_1(M_x + \ddot{r}_1 - r_1(\omega_y{}^2 + \omega_z{}^2)] + b_1[M_y + \omega_z\omega_x r_1 + 2\omega_z\dot{r}_1 + \dot{\omega}_z r_1] + c_1[M_z + \omega_z\omega_x r_1 - \omega_z\dot{r}_1 - \dot{\omega}_z r_1] \tag{30}$$

$$0_3 = a_3[M_x - \ddot{r}_1 + r_1(\omega_y{}^2 + \omega_z{}^2)] - b_3[M_y - \omega_y\omega_x r_1 - 2\omega_z r_1 - \dot{\omega}_z r_1] - c_1[M_z - \omega_z\omega_x r_1 + \omega_y\dot{r}_1 + \dot{\omega}_z r_1] \tag{31}$$

Antiparallelism has the advantage of rotational symmetry which simplifies the design and fabrication of fixtures. The outputs are converted to acceleration units by applying the appropriate gage factor P_i as follows,

$$G_i = \frac{0_i}{P_i} \tag{32}$$

which results in

$$G_1 = \frac{0_1}{P_1} = d_1[\ddot{M}_x - \ddot{r}_1 - r_1(\omega_y{}^2 + \omega_z{}^2)] + e_1[M_y + \omega_y\omega_x r_1 + 2\omega_z\dot{r}_1 + \dot{\omega}_z r_1] + f_1[M_z + \omega_z\omega_x r_1 - \omega_z\dot{r}_1 - \dot{\omega}_z r_1] \tag{33}$$

$$G_3 = \frac{0_3}{P_3} = d_3[M_x - \ddot{r}_1 + r_1(\omega_y{}^2 + \omega_z{}^2)] - e_3[M_y - \omega_y\omega_x r_1 + 2\omega_z\dot{r}_1 - \dot{\omega}_z r_1] - f_3[M_z - \omega_z\omega_x r_1 + \dot{\omega}_z\dot{r}_1 - \dot{\omega}_z r_1] \tag{34}$$

where

$$d_i = \frac{a_i}{P_i};\ e_i = \frac{b_i}{P_i},\ f_i = \frac{c_i}{P_i};$$

and

$$d_i=1;\ e_i=k_{1i},\ f_i=k_{2i};$$

or

$$d_i=k_{1i},\ e_i=k_{2i},\ f_i=1;$$

etc.

It can be shown that separating a specific vector component from the output of a single accelerometer is impossible, even if a perfectly uniaxial device is used. For example, if $d_{1=1}$ and $e_1 = f_1 = 0$,

$$G_1=a_1A_{1x}=\ddot{R}_x+\ddot{r}_1+\omega_x\omega_yR_y{}^2+\omega_x\omega_zR_z-(R_x+r_1)(\omega_y{}^2+\omega_z{}^2)+2\omega_y\dot{R}_z-2\omega_z\dot{R}_y+\dot{\omega}_zR_z-\dot{\omega}_zR_y \tag{35}$$

Modeling results and previous measurements show that the terms such as $(\omega_y\omega_xr_1)$ can be sufficiently large to demand attention. Also, the angular components in the other vector terms cannot be ignored.

In order to separate components, additional pairs of accelerometers must be used and the sums and differences of their data are required to separate vector components.

$$\frac{G_1-G_3}{2} = (\frac{d_1+d_3}{2})M_x + (\frac{e_1+e_3}{2})M_y + (\frac{f_1+f_3}{2})M_z +$$

$$+ (\frac{d_1-d_3}{2})(\ddot{r}-r(\omega_y{}^2+\omega_z{}^2) + (\frac{e_1-e_3}{2})(\omega_y\omega_x r+2\omega_z\dot{r}_1+\dot{\omega}_z r)$$

$$+ (\frac{f_1-f_3}{2})(\omega_z\omega_x r-2\omega_y\dot{r}-\dot{\omega}_y r) \tag{36}$$

$$\frac{G_1+G_3}{2} = (\frac{d_1+d_3}{2})(\ddot{r}-r(\omega_y{}^2+\omega_z{}^2) + (\frac{e_1+e_3}{2})(\omega_y\omega_x r+2\omega_z\dot{r}+\dot{\omega}_z r)$$

$$+ (\frac{f_1+f_3}{2})(\omega_z\omega_x r-2\omega_y\dot{r}-\dot{\omega}_y r) + (\frac{d_1-d_3}{2})\ddot{M}_x$$

$$+ (\frac{e_1-e_3}{2})M_y + (\frac{f_1-f_3}{2})M_z \; . \tag{37}$$

Upon examination of Eqs. (36) and (37), the advantage of having matched accelerometers becomes obvious. The commonality required is in the cross-axis sensitivity of the two devices. It becomes further evident that the lower the maximum cross-axis sensitivity, the better the separation among components.

When

$$\left.\begin{array}{l} d_1-d_3 \\ e_1-e_3 \\ f_1-f_3 \end{array}\right\} \rightarrow 0 \qquad \begin{array}{l} \dfrac{G_1-G_3}{2} \rightarrow d_1M_x + e_1M_y + f_1M_z \; . \\ \\ \dfrac{G_1+G_3}{2} \rightarrow d_1(\ddot{r}-r(\omega_y{}^2+\omega_z{}^2) + e_1(\omega_y\omega_x r+2\omega_z\dot{r}+\dot{\omega}_z r) \\ \qquad\qquad + f_1(\omega_z\omega_x r-2\omega_y\dot{r}-\dot{\omega}_y r) \end{array} \tag{38}$$

and as

$$\left.\begin{array}{l} k_1 \\ \\ k_2 \end{array}\right\} \to 0 \qquad \frac{G_1 - G_3}{2} \to \begin{array}{l} M_x \; ; \\ M_y \; ; \\ M_z \; ; \end{array}$$

$$\frac{G_1 + G_3}{2} \to (\ddot{r} - r(\omega_y{}^2 + \omega_z{}^2)) \; ,$$

$$(\omega_y \omega_x r + 2\omega_z \dot{r} + \dot{\omega}_z r) \; ,$$

$$(\omega_z \omega_x r - 2\omega_y \dot{r} - \omega_y r) \; . \qquad (39)$$

when d, e or f=1. Realistically, what is achievable is a pair of accelerometers with matched cross-axis sensitivity characteristics and maximum cross sensitivities less than 1%. That is, $k_{11} = k_{13}$, $k_{21} = k_{23}$ and we will continue our analysis based on

$$k_{1i} < .01,\ k_{11} \neq k_{13},\ k_{21} \neq k_{23},\ \text{and}\ k_{2i} < k_{1i}.$$

Since it is obvious that a single-pair array does not provide adequate definition of single vector components, multiple-pair arrays must be examined.

B. Multiple-Pair Arrays

Before examining and analyzing multiple-pair arrays, the acceleration vector at a point on the gun tube shown in Eq. (6) should be examined. To separate M_x, M_y and M_z, one can take advantage of the fact that these components do not vary with the local position vector component $\bar{r}$. This opens several options to the experimentor in placing accelerometer array pairs. The fact that the local angular acceleration components are directly dependent on $\bar{r}$ must be acknowledged when trying to separate rotational components. It should be noted that the components of $\bar{r}$ are factorable in the subsequent Eqs. (36) through (39). Eqs. (36) and (37) show that a minimum of three pairs is required in an array to unequivocally separate M_x, M_y and M_z, where each pair consists of matched accelerometers. The amount of mismatch of the cross-axis sensitivity in a given pair determines the error included in the data analysis. ω_x, ω_y and ω_z cannot be unequivocally separated in an array.

The multiple-pair array can be classified in three basic categories: colinear, coplanar and three-dimensionally distributed.

1. <u>Colinear Three-Pair Array</u>. The colinear three-pair array is shown in Figure 12. Basically, the origins of the coordinate systems of all six accelerometers lie on the same line, and their coordinate axes are parallel to the local coordinate axes with those in the upper position shown in Figure 12 coparallel and those in the lower position shown in Figure 12 antiparallel. In simpler terms, this array can be visualized as a pair of triaxial accelerometers mounted diametrically opposite one another on the gun tube with their respective axes opposing one another. For the indexing of positions, the first pair is at positions 1 and 3; the second pair is at positions 5 and 7; the third pair is at positions 9 and 11. The coefficients for the array are given in Table 5.

TABLE 5. COLINEAR THREE-PAIR ARRAY COEFFICIENTS

Position	d_i	e_i	f_i	r_i	P_i
1	1	k_{11}	k_{21}	r_1	P_1
3	1	k_{13}	k_{23}	$-r_1$	P_3
5	k_{25}	1	k_{15}	r_5	P_5
7	k_{27}	1	k_{17}	$-r_5$	P_7
9	k_{19}	k_{29}	1	r_9	P_9
11	k_{111}	k_{211}	1	$-r_9$	P_{11}

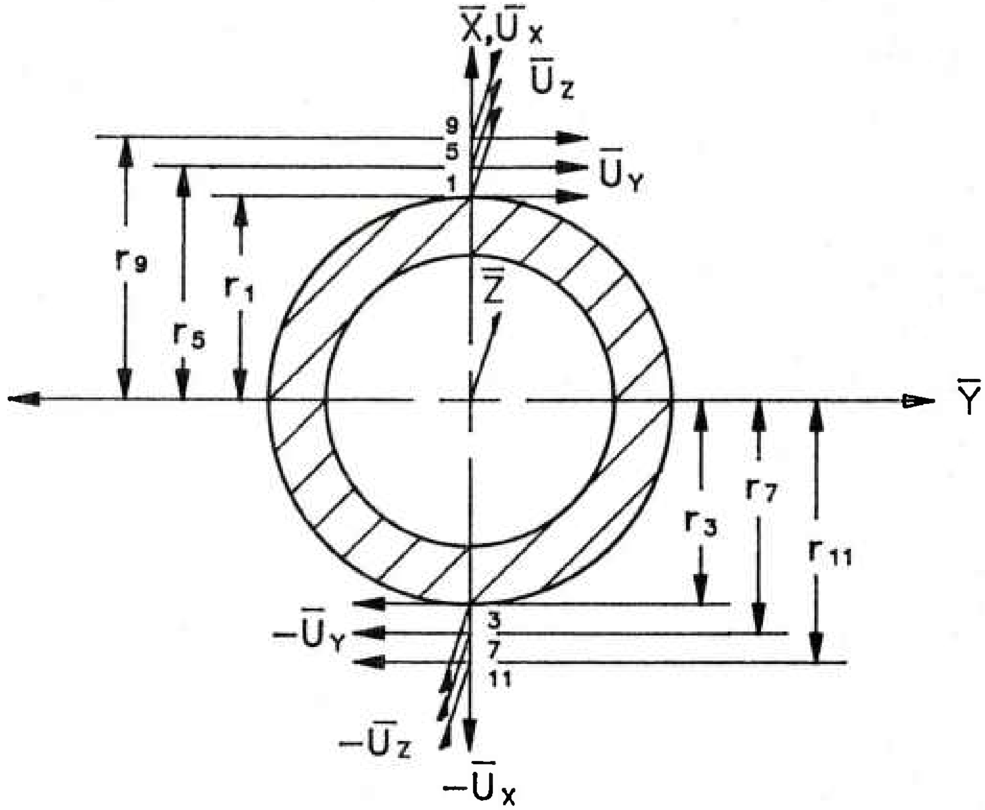

Figure 12. Colinear Three-Pair Array

The vector components M_x, M_y, M_z, $[\ddot{r}_1 - r_1(\omega_y^2 + \omega_z^2)]$, $[\omega_y \omega_x r_1 + 2\omega_z \dot{r}_1 + \dot{\omega}_z r_1]$ and $[\omega_z \omega_x r_1 - 2\omega_y \dot{r}_1 - \dot{\omega}_y r_1]$ can be found by taking the sums and differences of array pairs.

$$M_x = \frac{G_1 - G_3}{2} - \left(\frac{k_{11} + k_{13}}{2}\right) M_y - \left(\frac{k_{21} + k_{23}}{2}\right) M_z - \left(\frac{k_{21} - k_{23}}{2}\right)(\omega_z \omega_x r_1 - 2\omega_y \dot{r}_1 - \dot{\omega}_y r_1)$$

$$- \left(\frac{k_{11} - k_{13}}{2}\right)(\omega_y \omega_x r_1 + 2\omega_z \dot{r}_1 + \dot{\omega}_z r_1) .$$

$$M_y = \frac{G_5 - G_7}{2} - \left(\frac{k_{25} + k_{27}}{2}\right) M_x - \left(\frac{k_{15} + k_{17}}{2}\right) M_z + \left(\frac{k_{25} - k_{27}}{2}\right)(\ddot{r}_1 - r_5(\omega_y^2 + \omega_z^2))$$

$$- \left(\frac{k_{15} - k_{17}}{2}\right)(\omega_z \omega_x r_5 + 2\omega_y \dot{r}_5 + \dot{\omega}_y r_5) .$$

$$M_z = \frac{G_9-G_{11}}{2} - \left(\frac{k_{19}+k_{111}}{2}\right)M_x - \left(\frac{k_{29}+k_{211}}{2}\right)M_y + \left(\frac{k_{19}+k_{111}}{2}\right)\left(\ddot{r}_9 - r_9(\omega_y{}^2+\omega_z{}^2)\right)$$

$$- \left(\frac{k_{29}-k_{211}}{2}\right)(\omega_y\omega_x r_9 + 2\omega_z\dot{r}_9 + \dot{\omega}_z r_9) \quad .$$

$$\left(\ddot{r}_1 - r_1(\omega_y{}^2+\omega_z{}^2)\right) = -\frac{G_1+G_3}{2} + \left(\frac{k_{11}+k_{13}}{2}\right)(\omega_y\omega_x r_1 + 2\omega_z\dot{r}_1\omega r_1) + \left(\frac{k_{21}+k_{23}}{2}\right)(\omega_z\omega_x r_1 - 2\omega_y\dot{r}_1 - \dot{\omega}_y r_1)$$

$$+ \left(\frac{k_{11}-k_{13}}{2}\right)M_y + \left(\frac{k_{21}-k_{23}}{2}\right)M_z \quad .$$

$$(\omega_y\omega_x r_5 + 2\omega_z\dot{r}_5 + \dot{\omega}_z r_5) = -\frac{G_5+G_1}{2} + \left(\frac{k_{25}+k_{27}}{2}\right)\left(\ddot{r}_5 - r_5(\omega_y{}^2+\omega_z{}^2)\right) - \left(\frac{k_{15}+k_{17}}{2}\right)(\omega_z\omega_x r_5 - 2\omega_z\dot{r}_5 - \dot{\omega}_y r_5)$$

$$- \left(\frac{k_{25}-k_{27}}{2}\right)M_x - \left(\frac{k_{15}-k_{17}}{2}\right)M_z \quad .$$

$$(\omega_z\omega_x r_9 - 2\omega_y\dot{r}_9 - \dot{\omega}_y r_9) = \frac{G_9+G_{11}}{2} + \left(\frac{k_{19}+k_{111}}{2}\right) - \left(\ddot{r}_9 + r_9(\omega_y{}^2+\omega_z{}^2)\right)$$

$$- \frac{k_{29}+k_{211}}{2}(\omega_y\omega_x r_9 + 2\omega_z\dot{r}_9 + \dot{\omega}_z r_9) - \left(\frac{k_{19}-k_{111}}{2}\right)M_x - \left(\frac{k_{29}-k_{211}}{2}\right)M_y \quad . \qquad (40)$$

By substitution, Eqs. (40) become Eqs. (41) when

$$\frac{(k_{ij}+k_{ik})(k_{\ell m}+k_{\ell n})}{2} < .0001$$

and is considered to be zero for measurement purposes, and $\bar{r}$ is considered to be of constant magnitude

$$M_x = \tfrac{1}{2}\,G_1 - \tfrac{1}{2}\,G_3 - \left(\frac{(k_{11}+k_{13})+r_5+(k_{11}-k_{13})r_1}{4r_5}\right)G_5 - \left(\frac{(k_{11}-k_{13})r_1-(k_{11}+k_{13})r_5}{4r_5}\right)G_7$$

$$-\left(\frac{(k_{21}+k_{23})r_9+(k_{21}-k_{23})r_1}{4r_9}\right)G_9 - \left(\frac{(k_{21}-k_{23})r_1-(k_{21}+k_{23})r_9}{4r_9}\right)G_{11}\,.$$

$$M_y = -\left(\frac{(k_{25}+k_{22})r_7+(k_{25}-k_{27})r_5}{4r_1}\right)G_1 - \left(\frac{(k_{25}-k_{27})r_5-(k_{25}+k_{27})r_1}{4r_1}\right)G_3 + \tfrac{1}{2}\,G_5$$

$$-\tfrac{1}{2}\,G_7 - \left(\frac{(k_{15}+k_{17})r_9+(k_{15}-k_{17})r_5}{4r_9}\right)G_9 - \left(\frac{(k_{15}-k_{17})r_5-(k_{15}+k_{17})r_9}{4r_9}\right)G_{11}\,.$$

$$M_z = -\left(\frac{(k_{19}+k_{111})r_1+(k_{19}-k_{111})r_9}{4r_1}\right)G_1 - \left(\frac{(k_{19}-k_{111})r_9-(k_{19}+k_{111})r_1}{4r_1}\right)G_3$$

$$-\left(\frac{(k_{29}+k_{211})r_5+(k_{29}-k_{211})r_9}{4r_5}\right)G_5 - \left(\frac{(k_{29}-k_{211})r_9-(k_{29}+k_{211})r_5}{4r_5}\right)G_7 + \tfrac{1}{2}\,G_9 - \tfrac{1}{2}\,G_{11}$$

$$(\omega_y^{\,2}+\omega_z^{\,2}) = \frac{1}{r_1}\Big[-\tfrac{1}{2}\,G_1 - \tfrac{1}{2}\,G_3 + \left(\frac{(k_{11}+k_{13})r_1+(k_{11}-k_{13})r_5}{4r_5}\right)G_5 + \left(\frac{(k_{11}+k_{13})r_1-(k_{11}-k_{13})r_5}{4r_5}\right)G_7$$

$$+\left(\frac{(k_{21}+k_{23})r_1+(k_{21}-k_{23})r_9}{4r_9}\right)G_9 + \left(\frac{(k_{21}+k_{23})r_1-(k_{21}-k_{23})r_9}{4r_9}\right)G_{11}\Big]\,. \ *$$

$$(\omega_y\omega_x+\dot{\omega}_z) = \frac{1}{r_5}\Big[-\left(\frac{(k_{25}+k_{27})r_5+(k_{25}-k_{27})r_1}{4r_1}\right)G_1 - \left(\frac{(k_{25}+k_{27})r_5-(k_{25}-k_{27})r_1}{4r_1}\right)G_3 + \tfrac{1}{2}\,G_5$$

$$+\tfrac{1}{2}\,G_7 - \left(\frac{(k_{15}+k_{17})r_5+(k_{15}-k_{17})r_9}{4r_9}\right)G_9 - \left(\frac{(k_{15}+k_{17})r_5-(k_{15}-k_{17})r_9}{4r_9}\right)G_{11}\Big]\,. \ *$$

$$(\omega_z\omega_x-\dot{\omega}_y) = \frac{1}{r_9}\Big[-\left(\frac{(k_{19}+k_{111})r_9+(k_{19}-k_{111})r_1}{4r_1}\right)G_1 - \left(\frac{(k_{19}+k_{111})r_9-(k_{19}-k_{111})r_1}{4r_1}\right)G_3 + \tfrac{1}{2}\,G_{11}$$

$$-\left(\frac{(k_{29}+k_{211})r_9+(k_{29}-k_{211})r_5}{4r_5}\right)G_5-\left(\frac{(k_{29}+k_{211})r_9-(k_{29}-k_{211})r_5}{4r_5}\right)G_7+\tfrac{1}{2}\,G_9\Big] \; . \; * \tag{41}$$

*Not during projectile passage when $\ddot{r}$ and $\dot{r}$ exist

The results shown in Eqs. (41) are then used to establish the data processing algorithm.

2. Coplanar Three-Pair Array. It is not always physically possible to arrange accelerometers in a colinear array due to other physical constraints. Therefore, coplanar arrays must be considered. If an accelerometer is mounted on the surface of the tube at the end of the position vector $\bar{r}$ with one principal axis coparallel to $\bar{r}$ and the other principal axis coparallel to the tube axis, as shown in Figure 13, then the acceleration and sensitivity equations are:

$$\begin{aligned}\bar{A}_i = &\left\{[M_x+\ddot{r}_i+r_i(\omega_y{}^2+\omega_z{}^2)]\sin\phi_i + [M_y r_i\omega_y\omega_z+2\omega_z\dot{r}_i+\dot{\omega}_z r_i]\cos\phi_i\right\}\bar{U}_1\\ &+\left\{[M_y+r_i\omega_y\omega_z+2\omega_z\dot{r}_i+\dot{\omega}_z r_i]\,\sin\phi_i-[M_x+\ddot{r}_i+r_i(\omega_y{}^2+\omega_z{}^2)]\cos\phi_i\right\}\bar{U}_2\\ &+\left\{M_z+[\omega_z\omega_y r_i-2\omega_x\dot{r}_i-\dot{\omega}_x r_i]\cos\phi_i+[\omega_z\omega_x r_i-2\omega_y\dot{r}_i-\dot{\omega}_y r_i]\sin\phi_i\right\}\bar{U}_3;\end{aligned} \tag{42}$$

and

$$\frac{S_i}{P_i} = d_i\,\bar{U}_1 + e_i\,\bar{U}_2 + f_i\,\bar{U}_3 \tag{43}$$

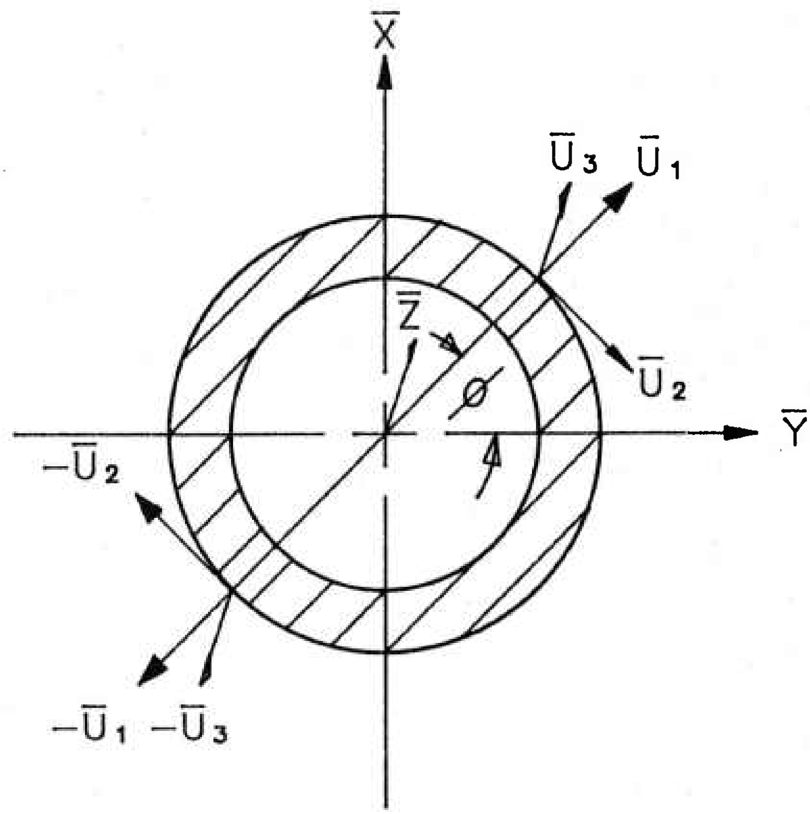

Figure 13. General Single-Pair Array

The array pair is completed by mounting an antiparallel mate in the diametrically opposite position i+2. The following general equations for the difference and sum are generated.

$$\frac{G_i - G_{i+2}}{2} = \frac{\bar{S}_i \cdot \bar{A}_i}{P_i} - \frac{\bar{S}_{i+2} \cdot \bar{A}_{i+2}}{P_{i+2}}$$

$$= \left[\frac{d_i \sin(\phi_i) - e_i \cos(\phi_i) + d_{i+2} \sin(\phi_i) - e_{i+2} \cos(\phi_i)}{2}\right] M_x$$

$$+ \left[\frac{d_i \cos(\phi_i) + e_i \sin(\phi_i) + d_{i+2} \cos(\phi_i) + e_{i+2} \sin(\phi_i)}{2}\right] M_y$$

$$+\left[\frac{(f_i+f_{i+2})}{2}\right]M_z$$

$$+\left[\frac{d_i\sin(d_j - e_i\cos(\phi_i) - d_{i+2}\sin(\phi_i) + e_{i+2}\cos(\phi_i)}{2}\right]\left[\ddot{r}_i + r_i(\omega_y{}^2 + \omega_z{}^2)\right]$$

$$+\left[\frac{d_i\cos(\phi_i) + 1e_i\sin(\phi_i) - d_{i+2}\cos(\phi_i) - e_{i+2}\sin(\phi_i)}{2}\right]\left[r_i\omega_y\omega_z + 2\omega_z\dot{r}_i + \dot{\omega}_z r_i\right]$$

$$+\left[\left(\frac{f_i - f_{i+2}}{2}\right)\sin\phi_i\right]\left[\omega_z\omega_x r_i - 2\omega_y\dot{r}_i - \dot{\omega}_y r_i\right]$$

$$+\left[\frac{(f_i - f_{i+2})}{2}\cos\phi_i\right]\left[\omega_z\omega_y r_i - 2\omega_x\dot{r}_i - \omega_x r_i\right] \qquad (44)$$

$$\frac{G_i + G_{i+2}}{2} = \frac{\bar{S}_i \cdot \bar{A}_i}{P_i} + \frac{\bar{S}_i \cdot \bar{A}_{i+2}}{P_i}$$

$$+\left[\frac{d_i\sin(\phi_i) - e_i\cos(\phi_i) + d_{i+2}\sin(\phi_i) - e_{i+2}\cos(\phi_i)}{2}\right]\left[\ddot{r}_i + r_i(\omega_y{}^2 + \omega_z{}^2\right]$$

$$+\left[\frac{d_i\cos(\phi_i) + e_i\sin(\phi_i) + d_{i+2}(\cos\phi_i) + e_{i+2}\sin(\phi_i)}{2}\right]\left[r_i\omega_y\omega_z + 2\omega_z\dot{r}_i + \dot{\omega}_z r_i\right]$$

$$+\left[\frac{f_i\sin(\phi_i) + f_{i+2}\sin(\phi_i)}{2}\right]\left[\omega_z\omega_x r_i - 2\omega_z\dot{r}_i - \dot{\omega}_z r_i\right]$$

$$+\left[\frac{f_i\cos(\phi_i) + f_{i+2}\cos(\phi_i)}{2}\right]\left[\omega_z\omega_y r_i - 2\omega_x\dot{r}_i - \dot{\omega}_x r_i\right]$$

$$+\left[\frac{f_i - f_{i+2}}{2}\right] M_z$$

$$+\left[\frac{d_i\sin(\phi_i) - e_i\cos(\phi_i) - d_{i+2}\sin(\phi_i) + e_{i+2}\cos(\phi_i)}{2}\right] M_x$$

$$+\left[\frac{d_i\cos(\phi_i) + e_i\sin(\phi_i) - d_{i+2}\cos(\phi_i) - e_{i+2}\sin(\phi_i)}{2}\right] M_y \qquad (45)$$

Figure 14 shows an example where the three-pair array is aligned with the coefficients given in Table 6.

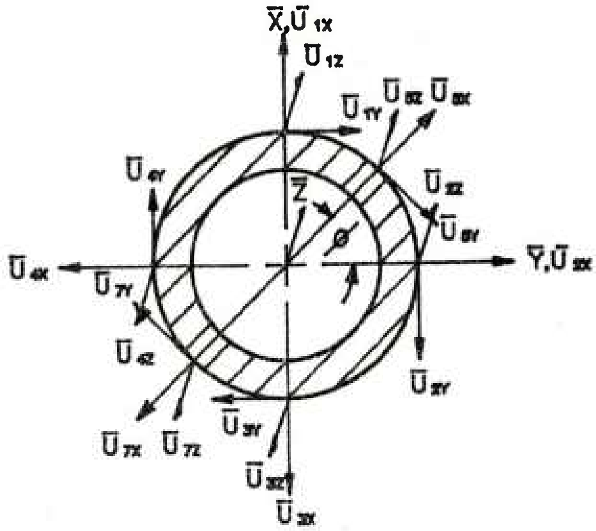

Figure 14. Coplanar Three-Pair Array

TABLE 6. COPLANAR THREE-PAIR ARRAY

Position i	i+2	d_i	e_i	f_i	r_i	ϕ_i
1		k_{21}	1	k_{11}	r_1	$\pi/2$
	3	k_{23}	1	k_{13}		
2		k_{22}	1	k_{12}	r_2	0
	4	k_{24}	1	k_{14}		
5		k_{15}	k_{25}	1	r_5	$\pi/4$
	7	k_{17}	k_{27}	1		

By substitution and recasting the difference of paired outputs

$$M_y = (\frac{G_1-G_3}{2})+(\frac{k_{21}+k_{23}}{2})(\frac{G_2-G_4}{2})-(\frac{k_{11}+k_{13}}{2})(\frac{G_5-G_7}{2})-(\frac{k_{21}-k_{23}}{2})[\ddot{r}_1+r_1(\omega_y{}^2+\omega_z{}^2)]$$

$$+ (\frac{k_{11}-k_{13}}{2})[\omega_z\omega_x r_1-2\omega_y\dot{r}_1-\dot{\omega}_y r_1];$$

$$M_x = -(\frac{G_2-G_4}{2})+(\frac{k_{22}+k_{24}}{2})(\frac{G_1-G_3}{2})+(\frac{k_{12}+k_{14}}{2})(\frac{G_5-G_7}{2})-(\frac{k_{22}-k_{24}}{2})(\ddot{r}_z-r(\omega_y{}^2+\omega_z{}^2)$$

$$+ (\frac{k_{12}-k_{14}}{2})(\omega_z\omega_x r_2+\dot{\omega}_x r_2)$$

$$M_z = (\frac{G_5-G_7}{2})+(\frac{.707}{2})(k_{15}-k_{25}+k_{17}-k_{27})(\frac{G_2-G_4}{2})-(\frac{.707}{2})(k_{15}+k_{25}+k_{17}+k_{27})(\frac{G_1-G_3}{2})$$

$$- (\frac{.707}{2})(k_{15}+k_{25}-k_{17}-k_{27})[r_5-\omega_y\omega_z r_5+2\omega_z\dot{r}_5+\dot{\omega}_z r_5]$$

$$- (\frac{.707}{2})(k_{15}-k_{25}-k_{17}+k_{27})[\ddot{r}_5+r_5(\omega_y{}^2+\omega_z{}^2)]$$

$$- (\frac{k_{11}+k_{13}}{2})r_1]; \qquad (46)$$

By closely examining the Eqs. (46), it is evident that M_y, M_x and M_z cannot be separated without residual error unless the corresponding accelerometer pairs are matched. The use of matched accelerometer pairs becomes a necessity for a coplanar array. Separation of angular terms cannot be readily done with real accelerometers. These terms depend on the maximum value of cross-axis sensitivities being much less than 1%, say less than .1%.

3. <u>Three-Dimensional Arrays.</u> The difficulties of separating vector components in three-dimensional arrays are compounded because of the physical restriction of being displaced from the central axis of the gun tube. In order to circumvent this situation, an approximate three-dimensional technique is used to determine $\dot{\omega}_x$ and $\dot{\omega}_y$ between two three-pair arrays.

Consider a segment of the gun tube as depicted in Figure 15 where the ends of the segment correspond to the locations of two array planes and M_x, M_y and M_z are defined in each plane. Also, the length L of the segment is sufficiently short to cause the angle ψ, the misalignment angle between the two planes, to be insignificant. Under these conditions, the rotations can be formulated as follows:

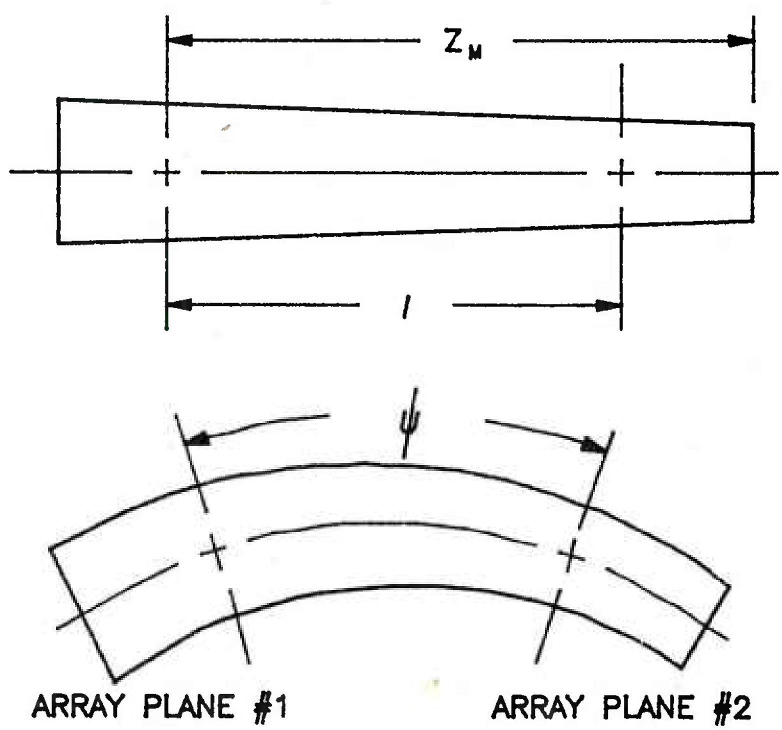

Figure 15. Three-Dimensional Array

$$\dot{\omega}_y = \frac{M_{x_2} - M_{x_1}}{L} , \tag{47}$$

$$\dot{\omega}_x = \frac{\ddot{M}_{y_2} - \ddot{M}_{y_1}}{L} . \tag{48}$$

Before Eqs. (47-48) can be used, the length L must be examined to insure that the previously stated assumption of sufficient shortness is not violated. The angle ψ can be expressed in terms of L based on the Bernoulli beam[7] equation

$$\frac{d^2x}{dz^2} = \frac{M_o}{EI} = \frac{8\ddot{R}\rho}{E(w^2+1)C^2}\,(z_m^2 - z)$$

$$\psi = \frac{dx}{dz} = \int_L^{z_m} \frac{M}{EI}\,dz = \frac{8\ddot{R}\rho}{E(w^2+1)C^2}\left(z_m^2 L - \frac{L^3}{3}\right) \tag{49}$$

where

I = cross-sectional moment of the tube at z;

M_o = moment on the tube at z;

E = modulus of elasticity;

ρ = density;

$\ddot{M}$ = average transverse acceleration;

C = caliber of the tube;

w = wall ratio of the tube;

z_m = distance from the primary array to the muzzle;

L = distance from the primary array to the secondary array;

---

[7] *Ferdinand L. Singer,* *Strength of Materials,* *Harper & Brothers, 1951.*

The constraint for the assumption is

$$\psi = \frac{8R\ddot{\rho}}{E(w^2+1)C^2}\left(z_m^2 L - \frac{L^3}{3}\right) < .001 \tag{50}$$

Eq. (50) reduces to

$$\left(z_m^2 L - \frac{L^3}{3}\right) < \frac{E(w^2+1)C^2}{8R\ddot{\rho}}(.001) \tag{51}$$

Experience tells us that over the range of caliber and wall ratios encountered z_m should not exceed 2.7 calibers and the minimum L should not be less than 0.5 caliber. The condition, inequality (51), has to be verified for each case. Eqs. (48) then are used in conjunction with the Eqs. (41) and (47), depending on the types of arrays used, to determine $\dot{\omega}_x$, $\dot{\omega}_y$ and $\dot{\omega}_z$.

V. TRANSFORMATION TO EARTH COORDINATES

In the previous discussion, the vector components are described in terms of the local coordinates of the gun tube. That is, in terms sensed by an observer on the gun tube. However, it is most convenient to describe the motion of elements of a gun system relative to an arbitrary Earth coordinate system. This type of description allows the determination of the relative motion between various components of the gun system.

A. Magnitude of Rotation Considerations

Before performing coordinate transformations, the rotational aspects of the motion must be examined.

$$\theta_x = \theta_{x_o} + \int_o^t \omega_{x_o}\, dt + \int_o^t\int_o^t \dot{\omega}_x\, dt\, dt;$$

$$\theta_y = \theta_{y_o} + \int_o^t \omega_{y_o}\, dt + \int_o^t\int_o^t \dot{\omega}_y\, dt\, dt;$$

$$\theta_z = \theta_{z_o} + \int_o^t \omega_{z_o}\, dt + \int_o^t \int_o^t \dot{\omega}_z\, dt\, dt \qquad (52)$$

where

θ_{i_o} = initial angular aspect;

ω_{i_o} = initial angular velocity;

$\dot{\omega}_i$ = instantaneous angular acceleration.

For most experiments the gun system is at rest at the time t=0. Consider Eqs. (52) where $\omega_{i_o} = 0$;

$$\theta_x = \theta_{x_o} + \int_o^t \int_o^t \dot{\omega}_x dt\, dt;$$

$$\theta_y = \theta_{y_o} + \int_o^t \int_o^t \dot{\omega}_y\, dt\, dt;$$

$$\theta_z = \theta_{z_o} + \int_o^t \int_o^t \dot{\omega}_z\, dt\, dt. \qquad (53)$$

If the absolute magnitudes of θ_x, θ_y and θ_z remain less than 0.06 radian, then an orthogonal transformation can be used. θ_{x_o}, θ_{y_o} and θ_{z_o} must be determined prior to the measurement by other means.

If the previously stated condition is violated, the transformation must be performed through the use of Euler angles, and the angular components must be redefined.[8]

[8] *Henry L. Langhaar, Energy Methods In Applied Mechanics, John Wiley and Sons, 1962.*

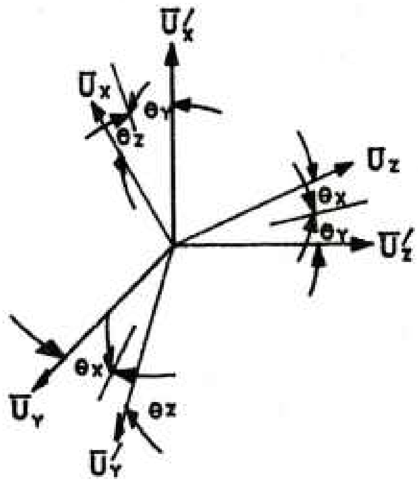

Figure 16. Orthogonal Transformation Angles

B. Orthogonal Transformation

Figure 16 shows the relationship between the local and Earth coordinates in terms of the orthogonal angles θ_x, θ_y and θ_z. Based on the condition that the absolute magnitudes of θ_x, θ_y and θ_z are less than 0.06 radian, the transformation matrix is shown in Table 7 where $\bar{f}(\bar{U}_x, \bar{U}_y, \bar{U}_z)$ is the local vector, and $\bar{F}(\bar{U}_x', \bar{U}_y', \bar{U}_z')$ is the Earth vector.

TABLE 7. ORTHOGONAL TRANSFORMATION COEFFICIENTS

	$\bar{U}_x$	$\bar{U}_y$	$\bar{U}_z$
$\bar{U}_x'$	1	$-\theta_z$	θ_y
$\bar{U}_y'$	θ_z	1	$-\theta_x$
$\bar{U}_z'$	$-\theta_y$	θ_x	1

$$\bar{M}' = M_x' \bar{U}_x' + M_y' \bar{U}_y' + M_z' \bar{U}_z' = (M_x - \theta_z M_y + \theta_y M_z)\bar{U}_x'$$

$$(M_y + \theta_z M_x - \theta_x M_z)\bar{U}_y' + (M_z - \theta_y M_x + \theta_x M_y)\bar{U}_z' \qquad (54)$$

The components of motion in the Earth coordinate system become

$$M_x' = (M_x - \theta_z M_y + \theta_y M_z) ;$$

$$M_y' = (M_y + \theta_z M_x - \theta_x M_z);$$

$$M_z' = (M_z - \theta_y M_x + \theta_y M_y) . \qquad (55)$$

$$\dot{\theta}_{x_o} = \dot{\theta}_{y_o} = \dot{\theta}_{z_o} = 0; \text{ when } t = 0.$$

$$\theta_{x_o} = A; \ \theta_{y_o} = B; \ \theta_{z_o} = C; \text{ when } t = 0.$$

C. Transformation By Euler Angles

Figure 17 shows two arbitrary coordinate systems rotated with respect to each other by the angles θ, ϕ and ψ. Table 8 shows the direction cosines between the unit vector of the coordinate systems. This matrix is valid as long as $\theta \neq 0$. Numerically, the transformation breaks down when θ is in the neighborhood of zero. By judicious selection of the coordinates, θ can be made to be always in the neighborhood of $\pi/2$.

TABLE 8. GENERAL EULER ANGLE TRANSFORMATION COEFFICIENTS

	ξ	η	ζ
x	$\sin(\phi)\sin(\psi)$ $-\cos(\theta)\cos(\phi)\cos(\psi)$	$\sin(\phi)\cos(\psi)$ $+\cos(\theta)\cos(\phi)\sin(\psi)$	$\sin(\theta)\cos(\phi)$
y	$-\cos(\phi)\sin(\psi)$ $-\cos(\theta)\sin(\phi)\cos(\psi)$	$-\cos(\phi)\cos(\psi)$ $+\cos(\theta)\sin(\phi)\sin(\psi)$	$\sin(\theta)\sin(\phi)$
z	$\sin(\theta)\cos(\psi)$	$-\sin(\theta)\sin(\psi)$	$\cos(\theta)$

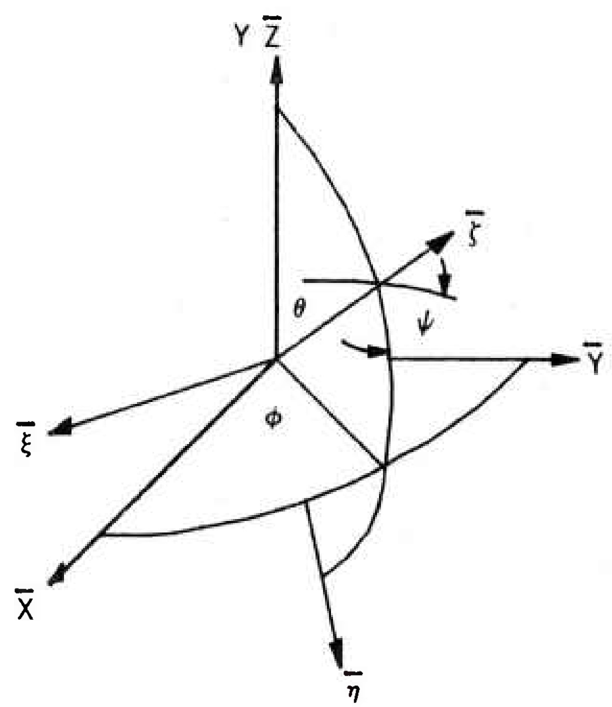

Figure 17. General Euler Angles

Figure 18 shows the coordinate systems for the desired transformation. A new table can be constructed by making the following substitutions.

$$\bar{U}_x' = \bar{z}, \quad \bar{U}_y' = \bar{x}, \quad \bar{U}_z' = \bar{y}$$

$$\bar{U}_x = -\bar{\eta}, \quad \bar{U}_y = \bar{\xi}, \quad \bar{U}_z = \zeta$$

$$\psi = \theta_z$$

$$\theta = \pi/2 - \theta_y \tag{56}$$

$$\phi = \pi/2 - \theta_x$$

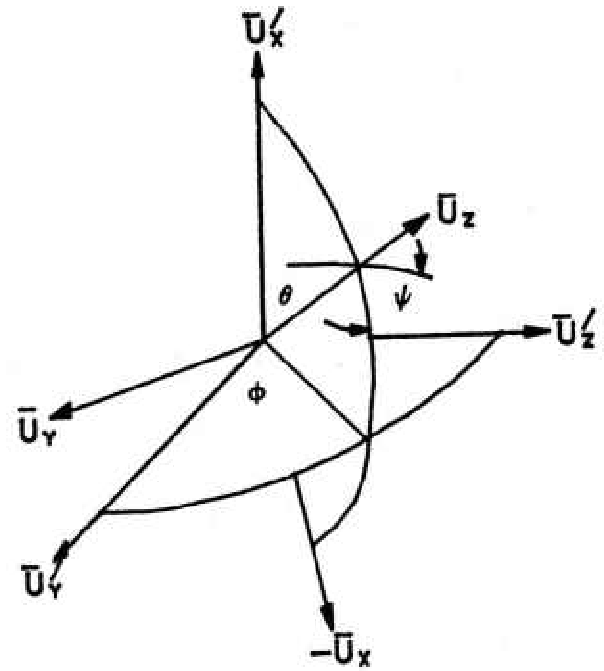

Figure 18. Euler Angle Transformation of Local and Earth Coordinates

Table 9 shows the new transform matrix after the Eq. (55) has been substituted in the matrix in Table 8.

D. Six-Degree-of-Freedom Measurement

On a gun tube, the six-degree-of-freedom measurement can be accomplished by using two colinear three-pair arrays.

1. Limitations. This measurement is limited to positions close to the muzzle.

2. Requirements. This measurement requires that the three-pair arrays be colinear. The positions of the two arrays conform to Eq. (51).

E. Linear Three-Degree-of-Freedom Measurements

The linear vectorial components of tube motion can be determined by using either colinear or coplanar arrays.

1. Limitations. Three-degree-of-freedom measurements do not allow transformation to Earth coordinates. Coplanar arrays can be used as well as colinear arrays, but must have matched pairs of accelerometers.

2. Requirements. Colinear arrays must have matched pairs of accelerometers. Positions and orientations must be well controlled and recorded.

F. Data Processing

As can be seen from the equations and conditions which must be used to make acceleration measurements, the subsequent processing should not be attempted without extensive automated facilities to digitize and numerically process massive amounts of data.

One of the most significant aspects of the analysis results is that data processing system bandwidth must accommodate the second harmonic of the highest mode frequency of the structural response. This means that digitization rates must be twenty times the highest response frequency of interest in order to adequately depict the six-degree-of-freedom motion of gun and projectile systems. This requirement also applies to the data rate and time step increment of numerical simulations of gun and projectile system response.

G. Comparison of Measurement and Theoretical Predictions

The primary result of the preceding analysis is that simulation outputs must be given in terms of the components that can exist in the measurand, not in the components historically used for mathematical convenience; that is

$$\ddot{R}_x+\omega_x\omega_y R_y+\omega_x\omega_z R_z-R_x(\omega_x{}^2+\dot{\omega}_y)+2\omega_y\dot{R}_z-2\omega_z\dot{R}_y+\dot{\omega}_y R_z-\dot{\omega}_z R_y=M_x$$

a viable measurand where

$$\ddot{R}_x$$

is not.

ACKNOWLEDGMENTS

The author wishes to express his appreciation for the persistence and excellence of Mrs. Janet Krokowski, who typed this report. Her ability and cheerful cooperation make a difficult task an enjoyable one.

REFERENCES

1. James N. Walbert, "Application of Digital Filters and the Fourier Transform to the Analysis of Ballistic Data," BRL Technical Report ARBRL-TR-02347, 1981 (ADA 102890).

2. James N. Walbert, "Computer Algorithms for the Design and Implementation of Linear Phase Finite Impulse Response Digital Filters," BRL Technical Report ARBRL-TR-02346, 1981 (ADA 103112).

3. James O. Pilcher II, "Application of Mechanical Filters to Ballistic Measurements," BRL Technical Report (to be published).

4. S.W. McCuskey, Introduction to Advanced Dynamics, Addison-Wesley Publishing Company, 1958.

5. Charles C. Crede and Cyril M. Harris, Shock and Vibration Handbook, Volume 1, McGraw-Hill, 1961.

6. Richmond B. McQuistan, Scalar and Vector Fields, John Wiley & Sons, 1965.

7. Ferdinand L. Singer, Strength of Materials, Harper & Brothers, 1951.

8. Henry L. Langhaar, Energy Methods In Applied Mechanics, John Wiley and Sons, 1962.

-

DISTRIBUTION LIST

No. of Copies	Organization
12	Administrator Defense Technical Info Center ATTN: DTIC-DDA Cameron Station Alexandria, VA 22314
1	Commander US Army Materiel Development and Readiness Command ATTN: DRCDMD-ST 5001 Eisenhower Avenue Alexandria, VA 22333
1	Commander US Army BMD Advanced Technology Center ATTN: BMDATC-M, Mr. P. Boyd P.O. Box 1500 Huntsville, AL 35804
1	Commander US Army Materiel Development and Readiness Command ATTN: DRCLDC, T. Shirata 5001 Eisenhower Avenue Alexandria, VA 22333
5	Commander USA ARRADCOM ATTN: DRDAR-TDC, Dr. D. Gyorog DRDAR-LC, Dr. J.T. Frasier DRDAR-SE DRDAR-SA DRDAR-AC Dover, NJ 07801
2	Commander USA ARRADCOM ATTN: DRDAR-TSS Dover, NJ 07801
6	Commander USA ARRADCOM ATTN: DRDAR-LCU, E. Barrieres DRDAR-LCU, R. Davitt DRDAR-LCU-M, D. Robertson DRDAR-LCU-M, J. Sikra DRDAR-LCU-M, M. Weinstock DRDAR-LCA, C. Larson Dover, NJ 07801
3	Commander USA ARRADCOM ATTN: DRDAR-LCA, B. Knutelski DRDAR-LCR-R, E-.H. Moore III DRDAR-LCS-D, K. Rubin Dover, NJ 07801
8	Commander USA ARRADCOM ATTN: DRDAR-SCM DRDAR-SCM, Dr. E. Bloore DRDAR-SCM, J. Mulherin DRDAR-SCS, B. Brodman DRDAR-SCS, Dr. T. Hung DRDAR-SCA, S. Jacobson DRDAR-SCA, W. Gadomski DRDAR-SCA, E. Malatesta Dover, NJ 07801
4	Commander USA ARRADCOM ATTN: DRDAR-LCR, W. Williver DRDAR-LCA, J. Reuben DRDAR-LCA, S. Bernstein DRDAR-LCN, G. Demitrack Dover, NJ 07801
4	Commander USA ARRADCOM ATTN: DRDAR-LCA, Dr. S. Yim DRDAR-LCA, L. Rosendorf DRDAR-LCA, Dr. S.H. Chu DRDAR-LCW, R. Wrenn Dover, NJ 07801
1	Director USA ARRADCOM Benet Weapons Laboratory ATTN: DRDAR-LCB-T Watervliet, NY 12189
2	Director USA ARRADCOM Benet Weapons Laboratory ATTN: DRDAR-LCB, Dr. T. Simkins DRDAR-LCB, Dr. J. Zweig Watervliet, NY 12189

DISTRIBUTION LIST

No. of Copies	Organization
1	Commander USA ARRADCOM ATTN: Product Assurance Directorate DRDAR-QA Dover, NJ 07801
1	Commander USA ARRADCOM ATTN: DRDAR-TSE, L. Goldsmith Dover, NJ 07801
1	Commander US Army Rock Island Arsenal ATTN: DRDAR-TSE-SW, R. Radkiewicz Rock Island, IL 61299
1	Commander US Army Armament Materiel Readiness Command ATTN: DRDAR-LEP-L, Tech Lib Rock Island, IL 61299
1	Commander US Army Aviation Research and Development Command ATTN: DRDAV-E 4300 Goodfellow Blvd. St. Louis, MO 63120
1	Director US Army Air Mobility Research and Development Laboratory Ames Research Center Moffett Field, CA 94035
1	Commander US Army Communications Research and Development Command ATTN: DRDCO-PPA-SA Fort Monmouth, NJ 07703
1	Commander US Army Electronics Research and Development Command Technical Support Activity ATTN: DELSD-L Fort Monmouth, NJ 07703
3	Commander US Army Harry Diamond Laboratories ATTN: DELHD-I-TR, H.D. Curchak DELHD-I-TR, H. Davis DELHD-S-OE-ES, B. Banner 2800 Powder Mill Road Adelphi, MD 20783
1	Commander US Army Harry Diamond Laboratories ATTN: DELHD-TA-L 2800 Powder Mill Road Adelphi, MD 20783
1	Commander US Army Missile Command ATTN: DRSMI-R Redstone Arsenal, AL 35898
1	Commander US Army Missile Command ATTN: DRSMI-YDL Redstone Arsenal, AL 35898
1	Commander US Army Tank Automotive Research and Development Command ATTN: DRDTA-UL Warren, MI 48090
2	Commander US Army Jefferson Proving Ground ATTN: STEJP-TD-O, A. Tilley STEJP-TD-E, J. Toomey Madison, IN 47251
1	Director US Army TRADOC Systems Analysis Activity ATTN: ATAA-SL, Tech Lib White Sands Missile Range, NM 88002
2	Commander US Army Yuma Proving Ground ATTN: STEYP-MTW, R. Torp G. Stullenbarger Yuma, AX 85364

DISTRIBUTION LIST

No. of Copies	Organization
2	Commander US Army Research Office ATTN: COL L. Mittenthal E. Saibel P.O. Box 12211 Research Triangle Park NC 27709
3	Commander US Army Research Office P.O. Box 12211 ATTN: Technical Director Engineering Division Metallurgy & Materials Division Research Triangle Park, NC 27709
2	Project Manager Nuclear Munitions ATTN: DRCPM-NUC Dover, NJ 07801
2	Project Manager Tank Main Armament Systems ATTN: DRCPM-TMA Dover, NJ 07801
2	Project Manager Division Air Defense Gun ATTN: DRCPM-ADG Dover, NJ 07801
3	Project Manager Cannon Artillery Weapons System ATTN: DRCPM-CAWS Dover, NJ 07801
1	Product Manager for 30mm Ammo. ATTN: DRCPM-AAH-30mm Dover, NJ 07801
2	Product Manager M110E2 Weapon System, DARCOM ATTN: DRCPM-M110E2 Rock Island, IL 61299

No. of Copies	Organization
2	Commander US Army Materials and Mechanics Research Center ATTN: J. Mescall Tech. Library Watertown, MA 02172
2	Commander Naval Sea Systems Command (SEA-03513) ATTN: L. Pasiuk Washington, DC 20362
1	Commander Naval Explosive Ordnance Disposal Facility ATTN: Lib Div Indian Head, MD 20640
1	Superintendent Naval Postgraduate School ATTN: Dir of Lib Monterey, CA 93940
1	Commander Naval Surface Weapons Center ATTN: G-13, W.D. Ralph Dahlgren, VA 22448
5	Commander Naval Surface Weapons Center ATTN: Code G-33, T.N. Tschirn Code N-43, J.J. Yagla L. Anderson G. Soo Hoo Code TX, Dr. W.G. Soper Dahlgren, VA 22448
2	Commander Naval Weapons Center ATTN: Code 3835, R. Sewell Code 3431, Tech Lib China Lake, CA 93555
2	Commander US Naval Weapons Center ATTN: Code 608, R. Derr Code 4505, C. Thelen China Lake, CA 93555

DISTRIBUTION LIST

No. of Copies	Organization
2	Commander Naval Ordnance Station ATTN: Code 5034, C. Irish, Jr. T.C. Smith Indian Head, MD 20640
4	AFATL Gun and Rocket Division Gun Test Branch AD3246 TEST W/TETFG ATTN: W. Dittrich; DLJM D. Davis; DLDL Eglin AFB, FL 32542
1	Southwest Research Institute ATTN: P. Cox 8500 Culebra Road San Antonio, TX 78228
1	AFELM, The Rand Corporation ATTN: Library-D 1700 Main Street Santa Monica, CA 90406

Aberdeen Proving Ground

Dir, USAMSAA
  ATTN: DRXSY-D
  DRXSY-MP, H. Cohen
Cdr, USATECOM
  ATTN: DRSTE-TO-F
Dir, USACSL
  Bldg. E3516, EA
  ATTN: DRDAR-CLB-PA
Dir, USAMTD
  ATTN: D. Dykstra
  J. Fasig
  S. Walton

USER EVALUATION OF REPORT

Please take a few minutes to answer the questions below; tear out this sheet, fold as indicated, staple or tape closed, and place in the mail. Your comments will provide us with information for improving future reports.

1. BRL Report Number_______________

2. Does this report satisfy a need? (Comment on purpose, related project, or other area of interest for which report will be used.)

____

____

____

3. How, specifically, is the report being used? (Information source, design data or procedure, management procedure, source of ideas, etc.)_______________

____

____

4. Has the information in this report led to any quantitative savings as far as man-hours/contract dollars saved, operating costs avoided, efficiencies achieved, etc.? If so, please elaborate.

____

____

5. General Comments (Indicate what you think should be changed to make this report and future reports of this type more responsive to your needs, more usable, improve readability, etc.)_______________

____

____

____

6. If you would like to be contacted by the personnel who prepared this report to raise specific questions or discuss the topic, please fill in the following information.

Name:_______________

Telephone Number:_______________

Organization Address:_______________

____

____